

## Applications of COSMIC to Meteorology and Climate

Richard A. Anthes<sup>1,\*</sup>, Christian Rocken<sup>2</sup>, Ying-Hwa Kuo<sup>3</sup>

(Manuscript received 20 May 1999, in final form 9 November 1999)

### ABSTRACT

The GPS/MET (Global Positioning System/Meteorology, Ware et al. 1996) project demonstrated atmospheric limb sounding from low-earth-orbit (LEO) with high vertical resolution, high accuracy, and global coverage in all weather. Based on the success and scientific results of GPS/MET, Taiwan's National Space Program Office (NSPO), the University Corporation for Atmospheric Research (UCAR), the Jet Propulsion Laboratory (JPL), the Naval Research Laboratory (NRL), the University of Texas at Austin, the University of Arizona, Florida State University and other partners in the university community are developing COSMIC (Constellation Observing System for Meteorology, Ionosphere and Climate), a follow-on project for weather and climate research, climate monitoring, space weather, and geodetic science. COSMIC plans to launch eight LEO satellites in 2004. Each COSMIC satellite will retrieve about 500 daily profiles of key ionospheric and atmospheric properties from the tracked GPS radio-signals as they are occulted behind the Earth limb. The constellation will provide frequent global snapshots of the atmosphere and ionosphere with about 4000 daily soundings.

This paper discusses some of the applications of COSMIC data for meteorology, including polar meteorology, numerical weather prediction (NWP), and climate. Applications to ionospheric research including space weather and geodesy are described elsewhere in this issue of TAO.

In meteorology COSMIC will provide high vertical resolution temperature, pressure and water vapor information for a variety of atmospheric process studies and improve the forecast accuracy of numerical weather prediction models. The COSMIC data set will allow investigation of the global water vapor distribution and map the atmospheric flow of water vapor that is so crucial for understanding and predicting weather and climate. The data set will provide accurate geopotential heights, enable the

---

<sup>1</sup>University Corporation for Atmospheric Research, Boulder, Colorado, USA

<sup>2</sup>GPS Science and Technology Program, UCAR, USA

<sup>3</sup>Mesoscale and Microscale Meteorology Division, National Center for Atmospheric, Research, UCAR

\* *Corresponding author address:* Dr. Richard A. Anthes, University Corporation for Atmospheric Research, P. O. Box 3000, Boulder, Colorado 80307, USA; E-mail: anthes@ucar.edu

detection of gravity waves from the upper troposphere to the stratosphere, reveal the height and shape of the tropopause globally with unprecedented accuracy, support the investigation of fronts and other baroclinic structures, and improve our understanding of tropopause-stratosphere exchange processes.

COSMIC data will complement other observing systems and improve global weather analyses, particularly over the oceans and polar regions, and NWP forecasts made from these analyses. Through assimilation in numerical models, COSMIC data will improve the resolution and accuracy of the global temperature, pressure and water vapor fields, and through the model's dynamical and physical adjustment mechanisms, the wind fields as well. These improved analyses and forecasts will provide significant benefits to aviation and other industries.

For climate research and monitoring COSMIC will provide an accurate global thermometer that will monitor Earth's atmosphere in all weather with unprecedented long-term stability, resolution, coverage, and accuracy. COSMIC will provide a data set for the detection of climate variability and change, the separation of natural and anthropogenic causes, the calibration of other satellite observing systems and the verification and improvement of climate models. COSMIC will contribute to studies of El Niño events especially in remote oceanic regions, and it will enable scientists to monitor the response of the global atmosphere to regional events such as volcanic eruptions, the Kuwait oil fires, or the recent Indonesian and Mexican forest fires. Upper-tropospheric refractivity data from COSMIC may shed new light on the controversy over the role that tropical convection plays in climate feedback. Global water vapor fields derived with the use of COSMIC data will provide new insights into the global hydrologic cycle.

**(Key words: Global Positioning System (GPS), GPS-Meteorology (GPS-MET), Remote sensing, Atmospheric sounding systems, Radio occultation, Atmospheric measurements, COSMIC (Constellation Observing System for Meteorology, Ionosphere and Climate)**

## **1. INTRODUCTION AND SUMMARY OF GPS/MET**

The Global Positioning System (GPS), established in prototype in the 1970s, and fully operational by the 1990s by the Department of Defense at a cost of approximately 15 billion U.S. dollars, is a satellite-based positioning system developed for navigation and positioning. More recently, civilian organizations from various nations have established the International GPS Service (IGS) network, which includes more than 100 globally distributed tracking stations and provides orbit determination with 5-cm accuracy in support of geodetic and geophysical research activities. The GPS today consists of 24 satellites that transmit L-band radio

signals (19 and 22 cm wavelengths) to a wide variety of users in navigation, time transfer and relative positioning and to an ever-increasing number of scientists in geodesy, atmospheric sciences, oceanography and hydrology. It is not an exaggeration to say that we are witnessing the beginnings of an explosion of scientific applications and discoveries using GPS for interdisciplinary studies in geosciences.

In atmospheric sciences, there are two primary methods by which GPS is being used to sense the atmosphere (Ware, 1992; Bevis et al., 1992; Businger et al., 1996). In the first method, dual-frequency GPS signals are collected at ground-based receivers and used to obtain the signal delay and thus the integrated water vapor along the path from the GPS satellites to the receiver (Rocken et al., 1993, 1995; Businger et al., 1996). In the second method, atmospheric soundings are obtained through the radio occultation technique, in which satellites in low-Earth orbit (LEO), as they rise and set relative to the GPS satellites, measure the change in frequency of the GPS dual-frequency signals. The Doppler-shifted frequency measurements are used to compute the bending angles of the radio waves, which are a function of atmospheric refractivity. The refractivity is a function of electron density in the ionosphere and temperature, pressure and water vapor in the neutral atmosphere. Hence the radio occultation measurement technique provides useful information about the structure of the ionosphere, stratosphere and troposphere.

The radio occultation sounding technique was developed by scientists at Stanford University and the Jet Propulsion Laboratory (JPL) for the remote sensing of planetary atmospheres (see review by Melbourne et al., 1994). The GPS/MET (GPS/Meteorology) program (Ware et al., 1996)<sup>4</sup> was established by the University Corporation for Atmospheric Research (UCAR) in 1993, joint with the University of Arizona and JPL, to demonstrate active limb sounding of the Earth's neutral atmosphere and ionosphere using the radio occultation technique. The demonstration system observed occulted GPS satellite signals received on a LEO satellite, MicroLab-1 (ML-1), launched April 3, 1995. From raw GPS/MET observations, vertical profiles of ray bending angle and refractivity were retrieved; from which ionospheric electron density, neutral atmospheric density, pressure, temperature, and moisture profiles were computed.<sup>5</sup> The program has been exceptionally successful, having accomplished nearly all of the "proof of concept" goals, plus a number of additional ones. As a direct result, GPS/MET technology is now widely recognized as a potential candidate for a new, accurate global observing system in support of weather prediction, climate change research and space weather.

---

<sup>4</sup>The GPS/MET Program was sponsored primarily by NSF, with additional funding provided by the Federal Aviation Administration (FAA) and the National Oceanic and Atmospheric Administration (NOAA). In addition, the National Aeronautics and Space Administration (NASA) provided significant "in kind support" via funding provided directly to JPL for support of GPS/MET. Orbital Sciences Corporation accommodated the GPS/MET payload on its MicroLab-1 Satellite and provided a Pegasus rocket launch. Allen Osborne Associates, Inc. worked with GPS/MET investigators to convert its commercial Turbo Rogue GPS receiver for use in space.

<sup>5</sup>The techniques, algorithms, and assumptions used to process GPS/MET observations are described by Hoeg et al. (1996), Kursinski et al. (1996, 1997), Hajj and Romans, 1998, Rocken et al. (1997), Hocke (1997) and Schreiner et al. 1999.

A summary of key GPS/MET results is presented in Table 1.

During and after the GPS/MET experiment, UCAR has made all data and related products freely available to the research community on the web.

The high theoretical accuracy of radio occultation soundings (Melbourne et al., 1994; Kursinski et al., 1997) was demonstrated in the GPS/MET experiment. Rocken et al. (1997) present statistical validation of GPS/MET data by comparing over 1,200 GPS/MET soundings of the troposphere and stratosphere to a variety of correlative data sets. Comparisons were carried out with NCEP (National Centers for Environmental Prediction) and ECMWF (European Centre for Medium-Range Weather Forecasting) analyses, radiosondes, and satellite data including GOES-8, TOVS (TIROS Operational Vertical Sounder), HALOE (Halogen Occultation Experiment) and MLS (Microwave Limb Sounder) instruments. Figure 1 summarizes the temperature comparison statistics.

The radio occultation method for obtaining atmospheric soundings is described elsewhere in this issue (Kursinski et al., 2000). Here it suffices to say that from the measured Doppler shift and the resulting bending angle data, vertical profiles of refractivity,  $N$ , can be derived. In the neutral atmosphere (stratosphere and troposphere), the bending angle-derived refractivity profiles are a function of temperature ( $T$  in K), pressure ( $P$  in mb), and water vapor pressure ( $e$  in mb),

$$N = 77.6 \frac{P}{T} + 3.73 \times 10^5 \frac{e}{T^2}. \quad (1)$$

Table 1. Summary of Results from GPS/MET Experiment.

<ul style="list-style-type: none"> <li>62,000 soundings were processed to level 1 (GPS phase, range and amplitude data), 11,000 processed to Level 3 (high-resolution profiles of temperature, pressure, refractivity, humidity, geopotential height) and published on the web. Several thousand soundings were compared to data from independent operational weather analyses and other observing systems.</li> </ul>
<ul style="list-style-type: none"> <li>The high theoretical temperature accuracy was verified (approximately 1K) in the range from the surface to 40 km.</li> </ul>
<ul style="list-style-type: none"> <li>Accurate retrieval of water vapor was demonstrated with use of ancillary temperature data.</li> </ul>
<ul style="list-style-type: none"> <li>High vertical resolution of approximately 500 m for sensing of the tropopause and upper level fronts was demonstrated.</li> </ul>
<ul style="list-style-type: none"> <li>All weather (including aerosols, clouds and precipitation) sounding capability was verified.</li> </ul>
<ul style="list-style-type: none"> <li>Determination of accurate geopotential heights of ~10 m was demonstrated.</li> </ul>
<ul style="list-style-type: none"> <li>Detection of gravity waves from the middle troposphere to stratosphere was demonstrated.</li> </ul>
<ul style="list-style-type: none"> <li>Accurate retrieval of vertical electron density profiles was demonstrated by ~10% level agreement with global ionosonde network foF2 data.</li> </ul>
<ul style="list-style-type: none"> <li>GPS/MET orbit data were used in the development of the new Earth Gravitational Model EGM96 (Lemoine et al., 1998).</li> </ul>
<ul style="list-style-type: none"> <li>Observing systems simulation experiments and real-data assimilation experiments have indicated a likely positive impact of GPS/MET data on model initialization and weather prediction.</li> </ul>
<ul style="list-style-type: none"> <li>A total of 123 data use agreements were issued for access through the GPS/MET web site, which still receives about 40,000 "hits"/month (<a href="http://cosmic.gpsmet.ucar.edu/gpsmet">http://cosmic.gpsmet.ucar.edu/gpsmet</a>)</li> </ul>
<ul style="list-style-type: none"> <li>The data have been used extensively and internationally for science and planning of follow-on missions.</li> </ul>
<ul style="list-style-type: none"> <li>More than 20 peer-reviewed publications have been written using the GPS/MET data.</li> </ul>

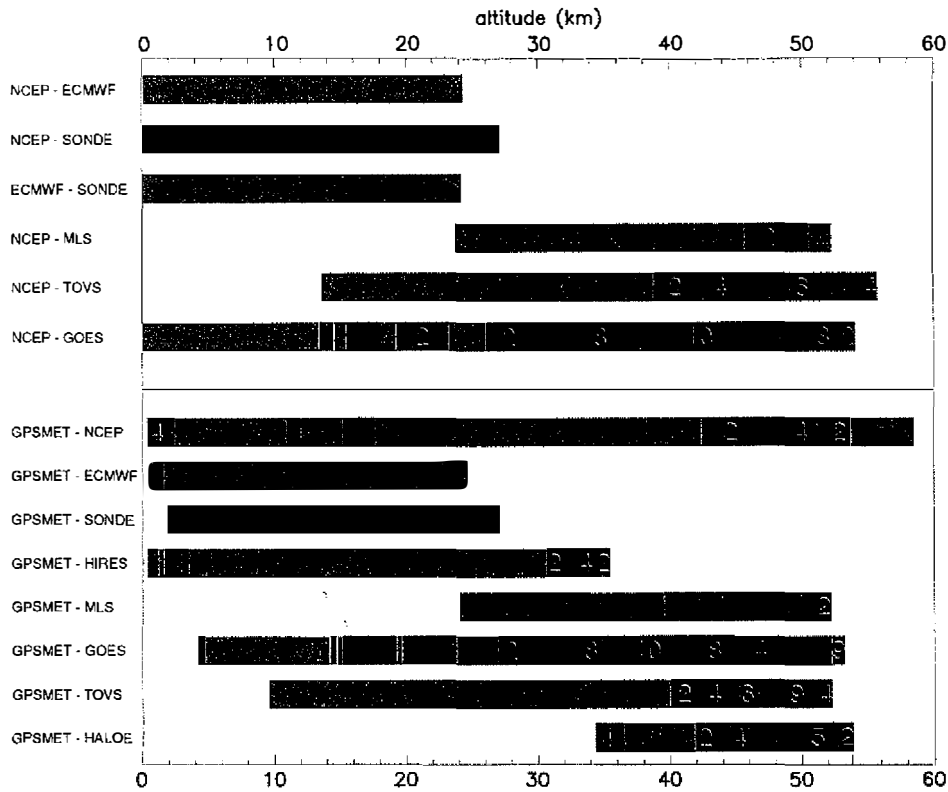


Fig. 1. Summary of temperature comparison statistics from Rocken et al. (1997) verification study. The upper six bars compare correlative temperature data and the lower 8 bars compare GPS/MET temperatures with correlative “dry” temperatures. “Dry” temperatures are computed from refractivity under the assumption of zero water vapor as discussed in more detail in section 2.2. Colors indicate altitude intervals of the comparisons. Regions where the average temperatures agree within  $\pm 1$  K are indicated in green. Positive average differences greater than 1 K are indicated in red; negative average differences less than -1 K are indicated in blue. The magnitude of the average differences is labeled where it occurs in degrees K. RMS differences about the mean are not shown here, but they are discussed in Rocken et al. 1997.

In the GPS/MET experiment, only setting occultations were observed and only about 10% of the soundings penetrated into the lowest kilometer of the atmosphere. The goal for COSMIC is to track 90% of all rising and setting occultation soundings to within one kilometer of the Earth’s surface. This will be achieved with (a)  $\sim 10$  db higher gain antennae and (b) with “open loop” tracking in the lower part of the troposphere (Meehan et al., 2000, personal communication).

Atmospheric inhomogeneities and multipath are the dominant error sources for profiles of refractivity below 20 km, obtained with the standard Abel inversion technique (Gorbunov and Gurvich, 1998). Resulting errors reach up to 10% near the surface (Kursinski et al., 1997). One way to avoid the error due to horizontal inhomogeneity, as discussed by Kuo et al. (2000) elsewhere in this journal, is to avoid the Abel inversion, and to assimilate profiles of bending angles into numerical weather models (Eyre, 1994; Zou et al., 1999). To minimize the errors due to multipath, the bending angles should be calculated after back-propagating of the received complex electromagnetic field closer to the limb, where the multipath effects are smaller (Gorbunov and Gurvich, 1998).

Unlike in-situ observations, a single radio occultation observation represents a fairly complicated average of atmospheric properties over a volume resembling a horizontal tube with an along-track horizontal scale of approximately 300 km and a radius of approximately 1 km (Fig. 1, Appendix A). Appendix A discusses this important issue of the spatial scales represented by radio occultation data, and distinguishes the concept of scale, or representativeness of a single observation, from resolution, which is a measure of the ability of a set of observations to define or analyze (resolve) atmospheric features of various horizontal and vertical scales. Appendix A also argues that the spatial scales represented by occultation soundings are ideal for use in global NWP models and for climate studies.

The characteristics of COSMIC data and their relevance to meteorology (including weather prediction) and climate are summarized in Table 2. The set of unique characteristics, including the accuracy and independence from all other observing systems, the fact that the retrieval process does not require a first-guess sounding, the absence of instrument drift and satellite-to-satellite bias and the ability to retrieve soundings in all weather (as shown by Solheim et al., 1999, the retrievals are minimally affected by clouds, aerosols or light precipitation), will make the COSMIC data very useful as complements to other observing systems. ESA (1996), Hoeg et al. (1996) and Melbourne et al. (1994) provide excellent discussions of the potential value of radio occultation data for meteorological and climate research and operations.

## 2. COSMIC AND METEOROLOGY

The characteristics of COSMIC data summarized above will make them valuable additions to the global observing system for a number of meteorological process studies, especially over the oceans and polar regions (Hoeg et al., 1996). The lack of accurate and high-resolution data over the oceans and polar regions, despite advances in operational satellite-based remote sensing capability, contributes much to the uncertainties in the initial state of weather-prediction models, which in turn limits the forecast skill of these models. With a total of 4,000 soundings per day, uniformly distributed around the globe, COSMIC will provide the much-needed additional data over data-sparse areas. The high vertical resolution, accurate, and independent COSMIC data will complement data from geostationary (Menzel et al., 1998) and polar-orbiting satellites, which provide high horizontal but low vertical resolution soundings. COSMIC represents a factor of four increase in terms of upper-air observations over the existing global radiosonde network, which has a total of ~900 stations (Fig. 2).

Table 2. Characteristics of COSMIC Data and Relevance to Meteorology and Climate Applications.

Characteristic	Meteorology	Climate
Limb sounding geometry complementary to ground and space nadir viewing instruments	X	X
High Accuracy	X	X
High vertical resolution	X	X
Consistency of horizontal and vertical scales of observations	X	X
All weather-minimally affected by clouds or precipitation	X	X
Independent height and pressure	X	X
Requires no first guess sounding	X	X
Independent of radiosonde or other calibration	X	X
No instrument drift		X
No satellite-to-satellite bias		X

The average horizontal spacing of the 4000 daily soundings shown in Fig. 2 varies with latitude, and is summarized in Fig. 3. The horizontal spacing is least near the poles (approximately 300 km) and greatest at the Equator (approximately 500 km).

The refractivity (or bending angle) profiles provide direct information on the horizontal and vertical structure of temperature and pressure fields in the stratosphere and middle and upper troposphere. Through continuous four-dimensional data assimilation, COSMIC data can be used to deduce information on the wind and water vapor fields, as shown by Kuo et al. (1997 and 2000, this issue) and discussed in section 3 of this paper. With improved description of temperature, pressure and wind fields, important signals on upper-troposphere baroclinic waves (which are the driver of surface cyclones and fronts, and their related weather) can be properly captured in the model initial conditions, even over the oceans and the other data-sparse regions. In the lower troposphere, COSMIC will contribute to the more accurate observation and analysis of water vapor, one of the most important atmospheric trace constituents. About 90% of severe weather is associated with clouds and precipitation. Unfortunately, water vapor, because of its inherent small-scale variations in time and space, is not well described by the existing observing systems, nor is it predicted well by the models. The assimilation of COSMIC data in operational NWP models will produce much improved description of the horizontal and vertical structure of water vapor on both global and regional scales. With these improvements, and supported by the recent results showing a positive impact of assimilating only three-layers of water vapor data from GOES 8/9 in NCEP's regional model (Menzel et al., 1998), we can anticipate a significant increase in forecast skill of precipitation and severe weather events.

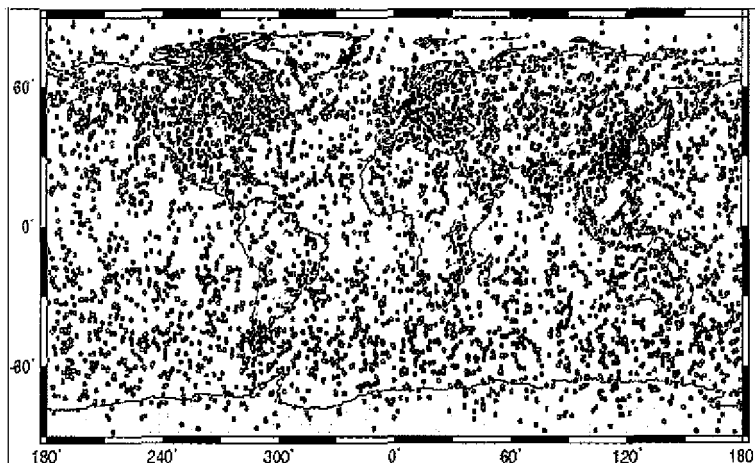


Fig. 2. Typical daily COSMIC soundings are shown in green, location of radio-sonde sites in red.

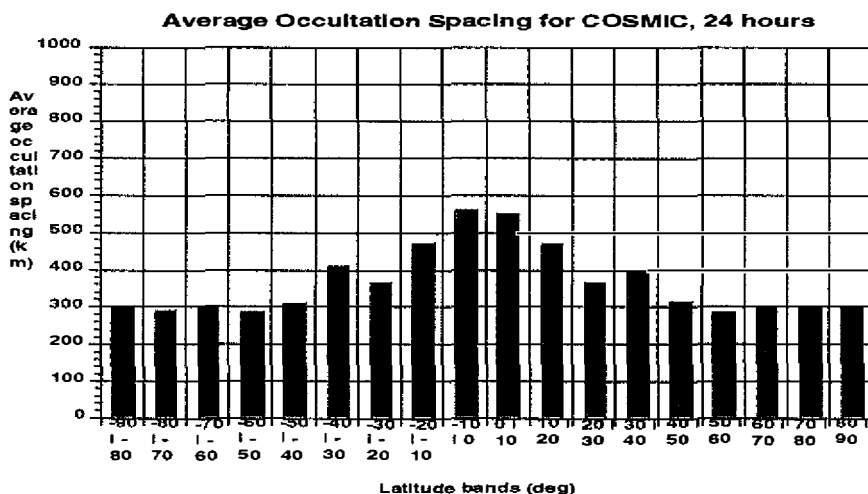


Fig. 3. Average spacing (km) between COSMIC soundings made over one day by 10-degree latitude bands.

## 2.1 Resolution of Important Atmospheric Structures

To be valuable for process studies and for NWP, COSMIC data must add additional information (beyond that already contributed by present observing systems) that resolves important features of the atmosphere. They must also contribute to the reduction of errors in the initial conditions of models that contribute most to forecast error growth. Palmer et al. (1998) discuss the use of singular vectors to study the sensitivity of models to initial errors. They point out that the vertical variation of the energy spectrum of the typical analysis error field is flatter



than that of the analysis itself. Thus, while the energy spectrum of the typical analysis field peaks near the tropopause, or jet-stream level, the energy spectrum of the analysis error field is more nearly constant throughout the tropopause. Similarly, the horizontal energy spectrum of analysis errors shows a flatter peak at smaller scales (e.g., wavenumbers 15-25, horizontal scales approximately 2,000 km) than does the analysis itself in which the peak is at planetary scales (wavenumbers 4-6, horizontal scales 7,000 - 10,000 km). From the structure of present analysis errors we expect COSMIC to be most useful in improving the initial structure of the atmosphere at relatively small (1,000-5,000 km) horizontal scales and from the lower troposphere into the lower stratosphere.

As shown in Fig. 3, the horizontal spacing of COSMIC data on a daily basis varies from approximately 300 km near the poles to 500 km in the tropics. In middle latitudes, the predominant features of interest are baroclinic waves and the associated cyclones and anticyclones. The horizontal wavelength of these waves varies from roughly 2,000 km for the shortest waves to 8,000 km for the long planetary waves. Wavenumbers 5-7 (wavelengths approximately 6,000-8,000 km) dominate the observed spectra (Staley and Gall, 1977; Holton, 1979). With an average spacing of approximately 300-400 km poleward of 20° latitude, COSMIC data will resolve these baroclinic waves well, especially when combined with other data. COSMIC data will also contribute to the observation and resolution of incipient baroclinic waves, especially over the oceans, because the wavelength of maximum baroclinic instability for typical conditions of static stability is about 4,000 km (Holton, 1979).

In the tropics, COSMIC data by themselves will not resolve the detailed structure of tropical cyclones with scales of typically several hundred kilometers. However, they will contribute significantly to the definition of the pressure, temperature and water vapor, and through data assimilation, the wind field in the large-scale environment surrounding the storm. The typical scale of circulation affecting the motion of tropical cyclones is 3,000-5,000 km from the cyclone center (Anthes, 1982; Pielke and Pielke, 1997). With a horizontal spacing of 350-450 km between latitudes 10° and 30°, COSMIC soundings will resolve the environment of the tropical storm and thereby contribute to improved tropical storm forecasts.

COSMIC data will resolve vertical scales as small as 0.5 km (Appendix A). This vertical resolution is considerably higher than satellite-based radiometric soundings. The GPS/MET experiment has indicated that the radio occultation soundings are capable of resolving strong temperature inversions associated with upper-level fronts and the tropopause (Kuo et al., 1998). The high accuracy and vertical resolution of COSMIC data in the upper troposphere and lower stratosphere should improve the analysis of potential vorticity in the vicinity of the jet stream and tropopause, a region known to be important in the accurate initialization of NWP models for predictions of cyclogenesis (Davis and Emanuel, 1991; Fehlmann and Davies, 1997).

Lindzen and Fox-Rabinovitz (1989) discuss the importance of having a consistency between the horizontal and vertical scales resolved by NWP models and observational systems. They show that most models and observational systems do not meet the consistency criteria over much of the Earth. Appendix A discusses this issue and shows that the horizontal and vertical scales of radio occultation data are close to meeting the consistency criteria; therefore COSMIC observations are expected to add significant value to the global observing system.

As noted earlier, many of the GPS/MET soundings did not penetrate into the lower 5 km

of the atmosphere. This was a limitation of the GPS/MET data because of the importance of the lower troposphere in weather prediction and climate. Not only is most of the atmosphere's water vapor located below 5 km, much of the atmospheric structure which is important in cyclogenesis occurs below 5 km. For example, Gelaro et al. (1998) show through construction of optimal perturbations using singular vector analysis that NWP models are most sensitive to small-scale baroclinic structures that have their maximum amplitude in the lower to middle troposphere. Observing system simulation experiments performed by Kuo et al. (1997) demonstrated the importance of GPS/MET data in the lower troposphere (below 3 km) for cyclone prediction. To realize the full potential of the radio occultation technique in improving numerical weather prediction and contributing to weather and climate studies, therefore, requires achieving the COSMIC goal of retrieving reliable soundings to at least within 1 km of the Earth's surface.

## 2.2 Retrieval of Temperature and Water Vapor

Given measurements of refractivity  $N$ , the relationship among refractivity, temperature, pressure and water vapor (Eq. 1), together with the hydrostatic equation, comprise a system of two equations with three unknowns. Equation (1) may be solved for either temperature  $T$  or water vapor pressure  $e$  given independent estimates of the other variable:

$$T = \frac{77.6 P + [6022.0 P^2 + 14.92 \times 10^5 eN]^{1/2}}{2N}, \quad (2)$$

and

$$e = \frac{T^2 N - 77.6 PT}{3.73 \times 10^5}. \quad (3)$$

Where water vapor is negligible, such as in the stratosphere and upper troposphere, pressure and temperature may be obtained directly from the refractivity ( $e=0$  in (2)). Temperatures retrieved with the assumption of zero water vapor are termed "dry temperatures" ( $T_{\text{dry}}$ ); the neglect of water vapor implies that  $T_{\text{dry}}$  is always less than or equal to  $T$ . Figure 4 shows comparisons of GPS/MET  $T_{\text{dry}}$  profiles with radiosonde temperatures in the tropics. There is excellent agreement between  $T_{\text{dry}}$  and the radiosonde temperatures between 10 and 35 km. Below 10 km the presence of water vapors causes  $T_{\text{dry}}$  to be less than the radiosonde temperature.

Where water vapor is present in significant amounts, it is impossible, without additional independent data, to separate out the effects of temperature and water vapor. However, in principle it is possible to calculate either water vapor or temperature given refractivity and the independent estimate of the other variable. In practice, it is much more likely that useful estimates of water vapor can be obtained given the refractivity and an independent estimate of temperature than the other way around. This can be seen by the relationship between errors in calculating temperature and water vapor from refractivity given independent estimates of water vapor and temperature. As shown by Ware et al. (1996), the relationship between errors in temperature and water vapor pressure, under the assumption of no errors in  $N$  or  $P$ , is

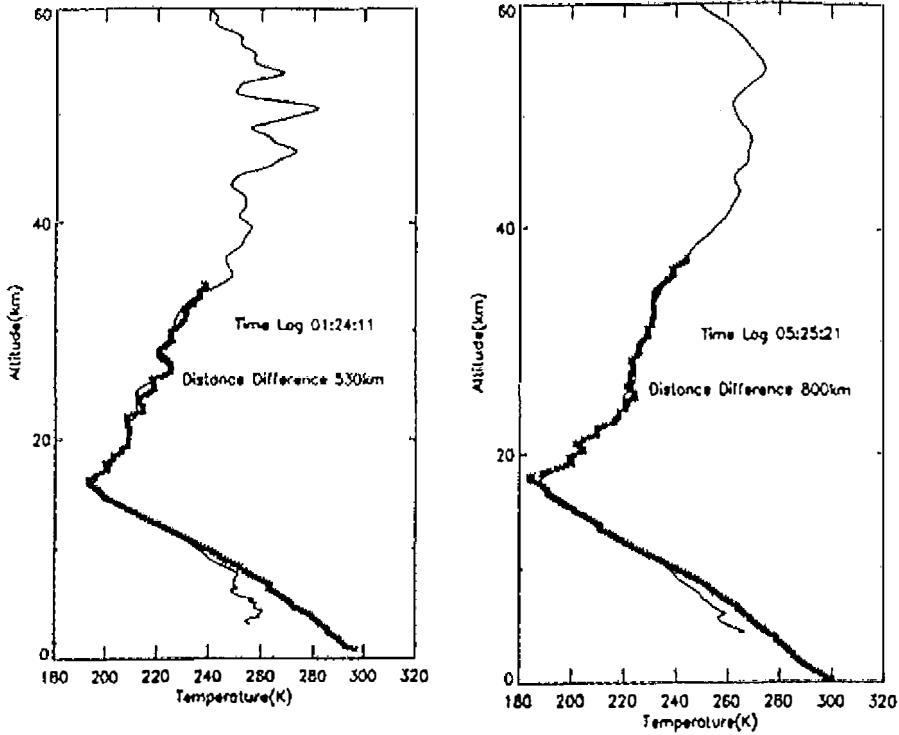


Fig. 4. Comparison of dry temperature profiles from GPS/MET (thin line) and nearby radiosonde (thick line) temperatures at Bandung (6.9°S, 107.6°E) and Pontianak (0.03°N, 109.3°E) in Indonesia on July 9, 1995 and January 10, 1997. The GPS/MET soundings are located at 2.92°S, 111.55°E and 8.30°S, 110.91°E respectively. The time lag and distance difference between the GPS/MET soundings and the radiosondes are indicated in the figure. (Professor Toshitaka Tsuda, Kyoto University, personal communication)

$$\Delta e \approx \frac{(2TN - 77.6P)}{3.73 \times 10^5} \Delta T. \quad (4)$$

For typical values of  $N=300$ ,  $P=1000$  mb, and  $T=273$ K we have

$$\Delta e \approx 0.23\Delta T, \text{ or } \Delta T \approx 4.35\Delta e. \quad (5)$$

The above error equations show that water vapor must be independently known to a very high accuracy if useful estimates of temperature from refractivity are to be obtained. Specifically,  $e$  would have to be known to within an accuracy of at least 0.23 mb to obtain temperature estimates accurate to within 1 K. However, if temperature is known independently to within an accuracy of 2 K, estimates of water vapor pressure can be determined with an accu-

racy of about 0.5 mb. This would be a useful estimate in many regions of the lower troposphere where water vapor typically varies between 5 and 20 mb and other measurements of water vapor are unavailable. Thus, if a reasonably accurate independent estimate of temperature is available (e.g., from a global analysis or a 12-hour forecast), accurate profiles of water vapor can be obtained<sup>6</sup> (Fig. 5). Gorbunov et al. (1996a,b) discuss alternative ways of estimating water vapor and temperature from refractivity and show examples of accurate retrievals of water vapor using simulated radio occultation measurements and output from a general circulation model.

### 2.3 Upper Level Fronts and the Tropopause

As demonstrated by GPS/MET, COSMIC data will provide high-vertical resolution data that can contribute significantly to the observation and analysis of atmospheric fronts and the tropopause. Kuo et al. (1998) showed that GPS/MET data accurately resolved an intense upper-level front over China (Fig. 6), and that even though this front occurred in a region of dense radiosonde data, the operational analyses of NCEP and ECMWF resolved this front only in a very smooth way.

GPS/MET data have resolved other upper-level fronts, as shown in the following two previously unpublished examples. Figure 7 shows a GPS/MET sounding taken at 08:11 UTC 14 October 1995 at a location just north of Lake Huron near Sudbury, Ontario (47°N 81°W).

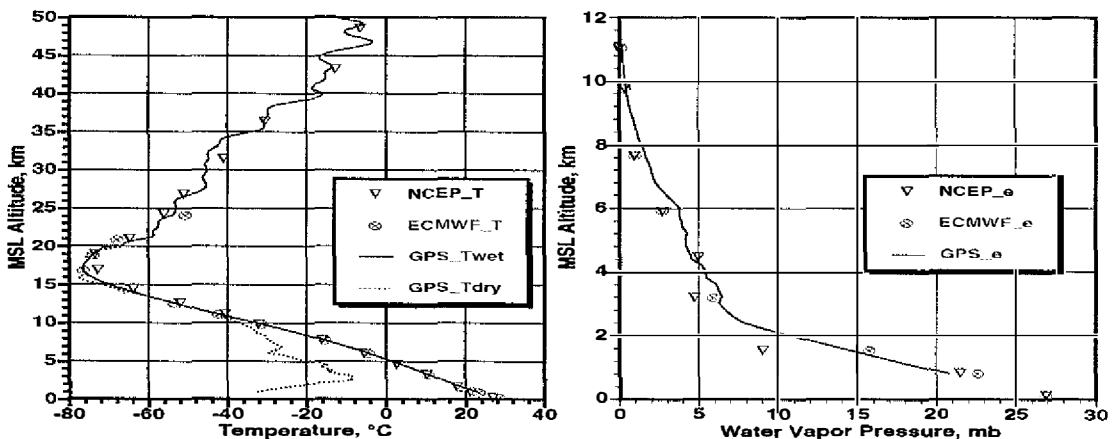


Fig. 5. GPS/MET occultation profiles from 11:40 UTC on June 22, 1995 at 9°S, 172°W compared with global analyses from NCEP and ECMWF (Rocken et al., 1997).

<sup>6</sup>The situation is somewhat different in the upper troposphere, where the saturation water vapor pressure is small, and much more accurate estimates of temperature are necessary to obtain useful estimates of water vapor pressure (Kursinski et al. 1996). For example, for a standard atmosphere at 300 mb (approximately 7 km),  $T \approx 243\text{K}$ ,  $e_s \approx 0.5\text{mb}$ ,  $N \approx 100$  and  $\Delta e \approx 0.07 \Delta T$ . Here a 1 K error in  $T$  produces an error in  $e$  that is a significant fraction of  $e_s$ .

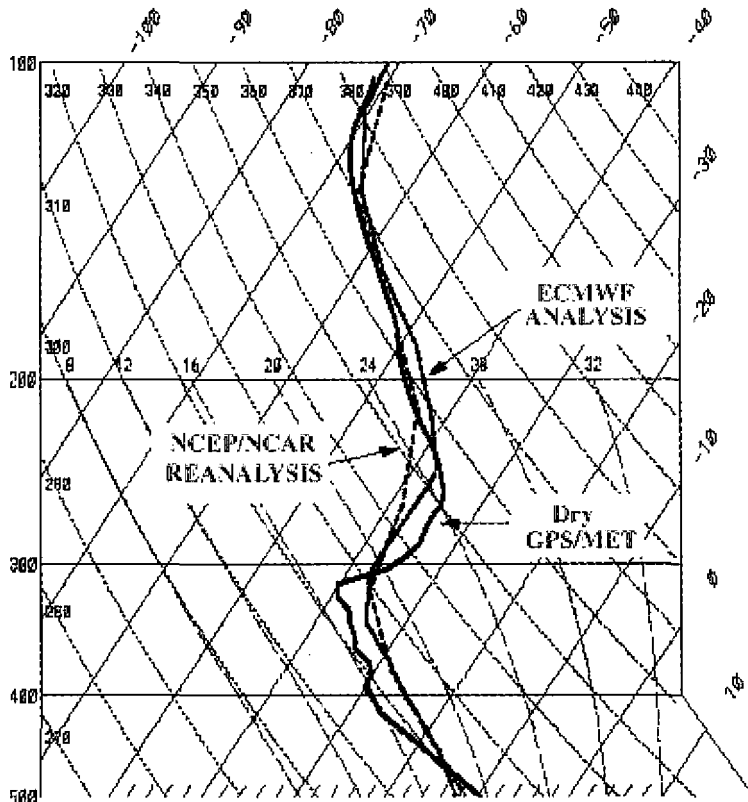


Fig. 6. Comparison of GPS/MET temperature sounding over China and the NCEP and ECMWF analyses interpolated to the GPS/MET sounding location at 00:00 UTC October 22, 1995 (Kuo et al., 1998).

An inversion of about 2 K is present at about 7.5 km (approximately 400 mb). The inversion is not present in either the ECMWF or the NCEP analyses. The 400-mb analysis for 12:00 UTC 14 October (Fig. 8) shows a trough centered over Wisconsin with a strong baroclinic zone ahead of the trough. The GPS/MET sounding is located near the leading edge of the baroclinic zone in a region of modest temperature gradient.

A third example of an upper-level front is shown in Fig. 9. This front, located about 750 km west of Los Angeles ( $31.2^{\circ}$  N  $135.3^{\circ}$  W), was observed at 22:54 UTC 8 February 1997 in advance of an upper-level trough (not shown). It shows a temperature inversion between 11 and 12 km of approximately 7 K, and again, this inversion is not present in the NCEP and ECMWF analyses.

COSMIC soundings will improve the resolution of the tropopause over the world. Figure 10 illustrates the capability of the radio occultation technique to resolve the tropopause with higher resolution than TOVS data, and also higher than that typically achieved by operational analyses, which depend heavily on TOVS data in regions where radiosondes are not present. Other examples of soundings that resolve the tropopause very well are shown in Fig. 11.

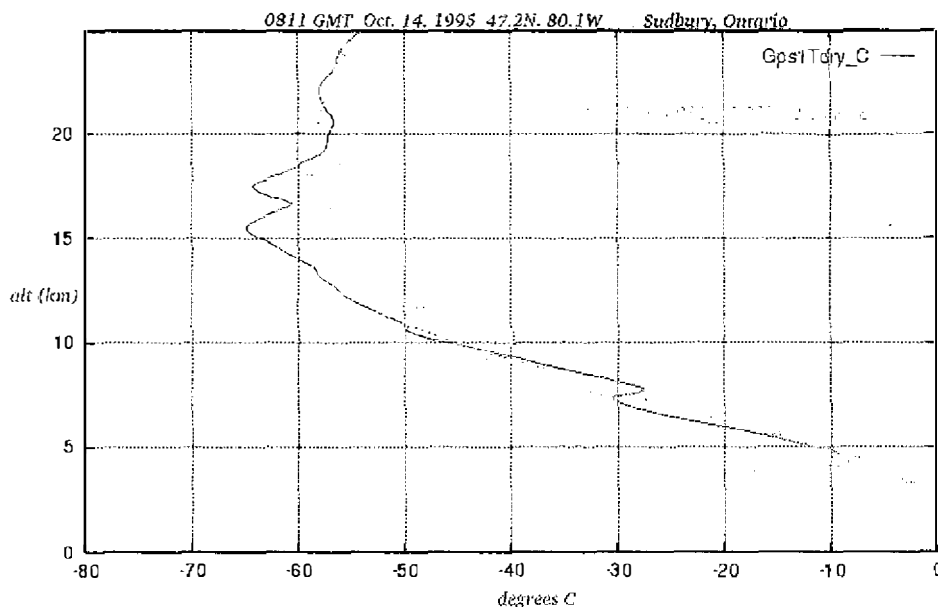


Fig. 7. Comparison of GPS/MET temperature sounding (solid line) at 08:11 UTC October 14, 1995 and 47.2°N, 80.1°W with NCEP and ECMWF 12:00 UTC analysis temperatures interpolated to the GPS/MET location. Also shown are data from a radiosonde (green diamonds) located at 46°N, 84°W at 12:00 UTC.

## 2.4 Gravity Waves and Stratospheric Dynamics

As summarized in the planning document for the SPARC (Stratospheric Processes and their Role in Climate) Program (WCRP, 1998), the stratosphere plays an important role in weather and climate. COSMIC data will contribute strongly to the SPARC goals of understanding stratosphere-troposphere exchange and the structure and climatology of stratospheric gravity waves and their parameterization in NWP and climate models (ESA, 1996).

Hocke (1997) describes the use of GPS/MET data for the study of gravity waves in the middle and upper atmosphere. For example, Kursinski et al. (1996) show a GPS/MET temperature sounding with oscillations in the stratosphere of vertical wavelengths around 3 km; these waves were in excellent agreement with waves resolved by a nearby radiosonde. The vertical oscillations shown in Fig. 4 above about 35 km and in Fig. 12 above 40 km are likely due to gravity waves.

Tsuda et al. (2000) have used the temperature variance of individual GPS/MET profiles, which is assumed to be caused by gravity waves, to compute the potential energy  $E_p$ . They found that GPS/MET derived  $E_p$  around Japan shows a seasonal variation with enhancement in the winter months, which is consistent with several years of radar observations. They also generated a global map of  $E_p$  from winter (Nov 96-Feb 97) GPS/MET soundings. These results are shown in Fig. 13, and they strongly suggest that atmospheric gravity waves are

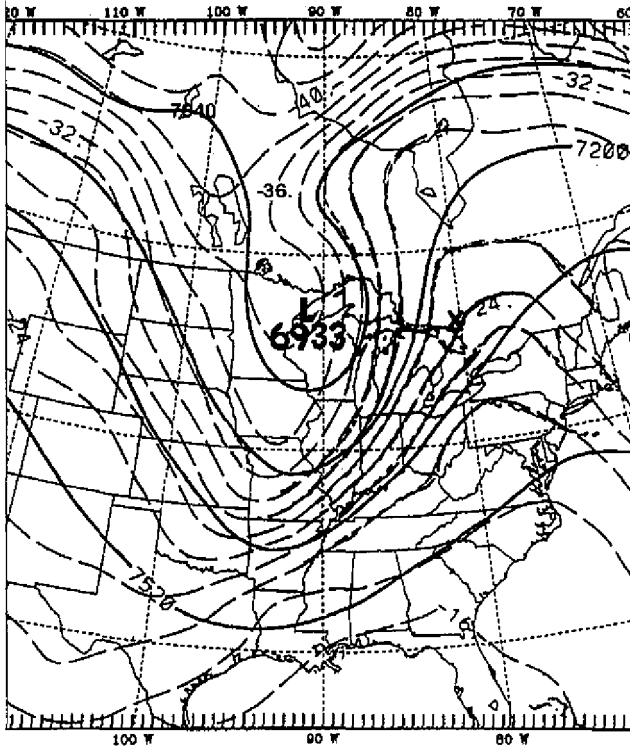


Fig. 8. Geopotential heights (solid lines, contour interval 160 m) and temperature (dashed lines, contour interval 2 K) from NCEP analysis at 12:00 UTC October 14, 1995. The symbol  $x$  just north of Lake Huron marks the location of the GPS/MET sounding.

generated by convection in tropical regions, particularly over the Indonesia archipelago, the Indian Ocean, Africa and the eastern Atlantic and South America. COSMIC promises to detect gravity wave activity globally with much better temporal and spatial resolution, thus allowing studies of how gravity waves relate to wind shear, thunderstorms, cyclones and other meteorological phenomena.

## 2.5 Polar Meteorology

COSMIC will greatly increase the amount of atmospheric soundings in the polar regions where operational analyses often show large errors (e.g., Fig. 11). Figure 14 shows the expected soundings from 8 satellites in one day. These data will contribute to polar science in a variety of ways.

Duck et al. (1998) report observations of annual late December warming of the upper stratosphere in the Arctic polar vortex. This warming, which extended into the lower stratosphere and which was accompanied by increased gravity wave activity, is important to understanding ozone depletion. Ozone depletion is sensitive to temperatures within the arctic vortex (Schoeberl and Hartmann, 1991). Dense and accurate temperature and gravity wave observations from COSMIC will help to reach an improved understanding of detailed processes controlling intra-vortex stratospheric temperatures, and will lead to improvements in Global Circulation Models (GCMs). Such improvements may enable GCMs to produce reliable predictions of the future state of the ozone layer (Duck et al., 1998).

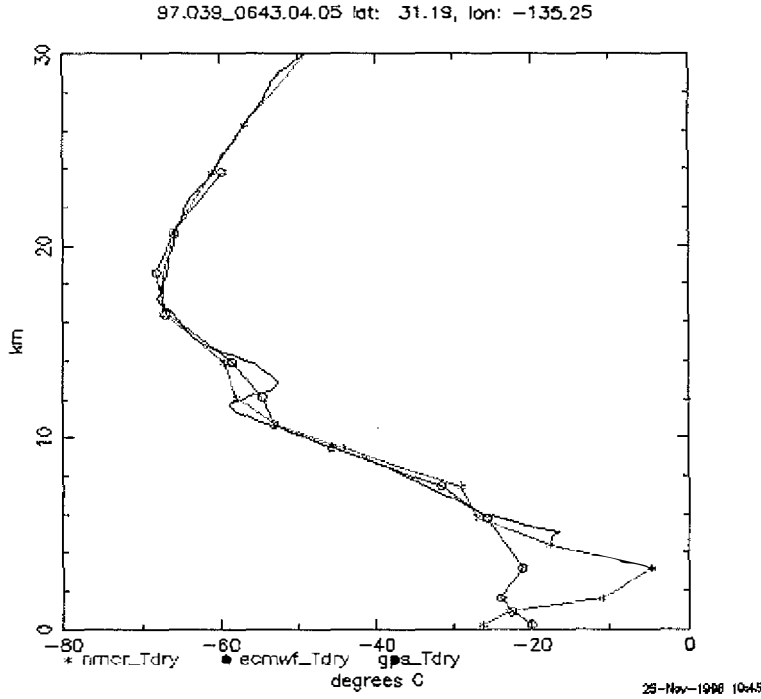


Fig. 9. Comparison of GPS/MET temperature sounding at 22:54 UTC Feb. 8, 1997 and 31.2°N, 135.3°W with NCEP and ECMWF 00:00 UTC February 9, 1997 analysis temperatures interpolated to the GPS/MET location.

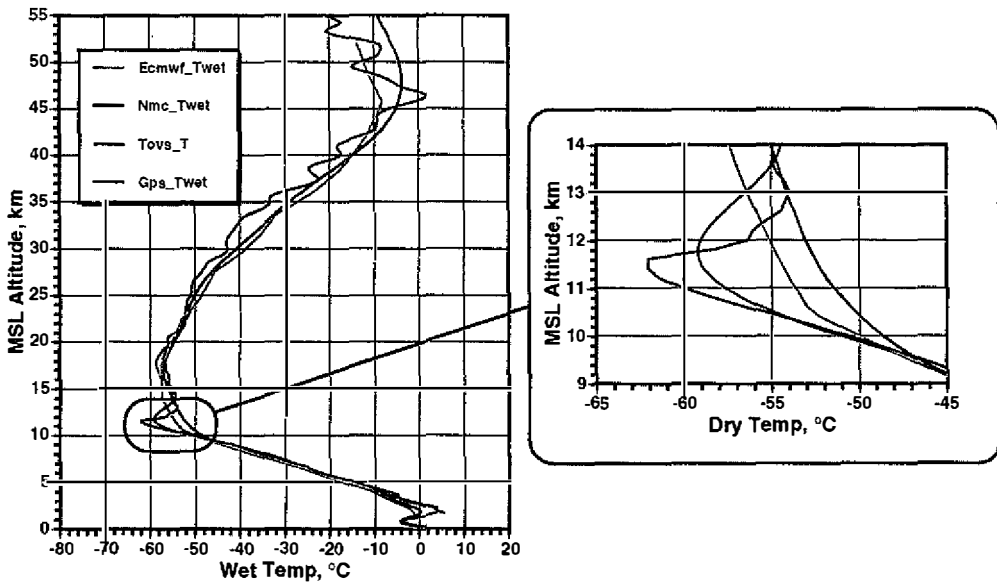


Fig. 10. Comparison of GPS/MET temperature sounding at 17:24 UTC October 21, 1995 and 47.0°S, 59.3°E with NCEP and ECMWF 00:00 UTC October 22, 1995 analysis temperatures interpolated to the GPS/MET location. Also shown is a nearby TOVS sounding.



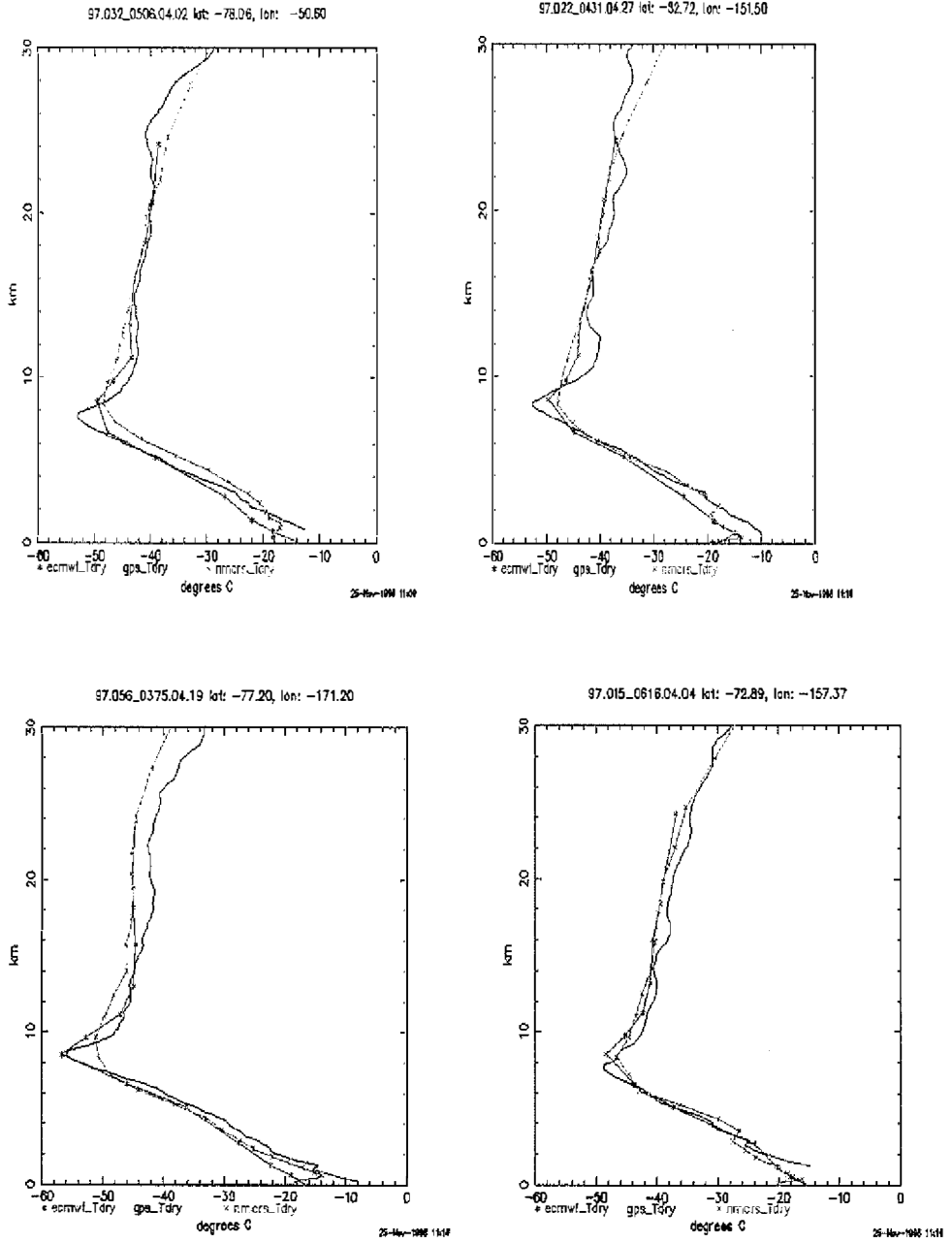


Fig. 11. Comparison of GPS/MET temperature soundings (solid blue lines) at four times and locations in January and February 1997 near Antarctica with NCEP and ECMWF analysis temperatures interpolated to the GPS/MET locations. Note the large discrepancy at and above the tropopause. We attribute these differences to analysis errors.

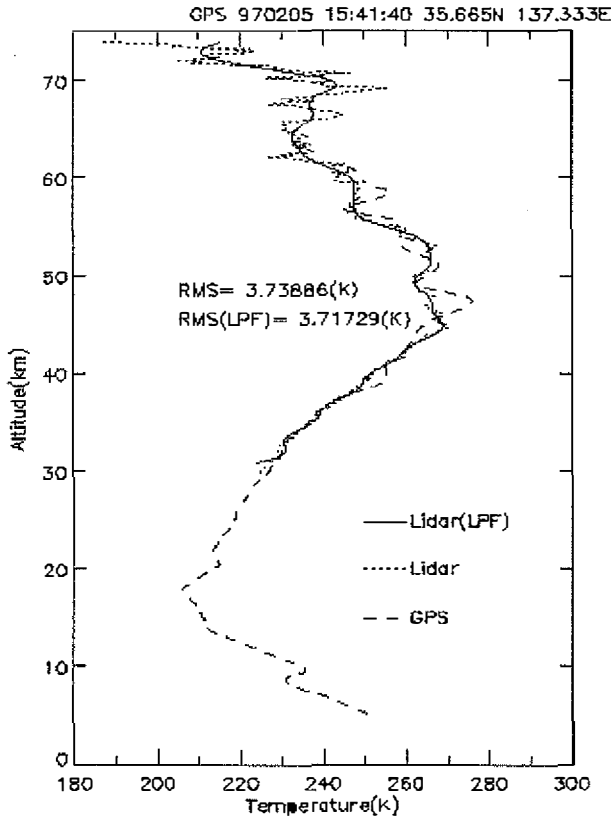


Fig. 12. Comparison of temperature profiles between GPS/MET data (dashed lines) at 15:41 UTC February 5, 1997 at 35.7°N, 137.3°E and Rayleigh lidar data (dotted line) between 15:08 and 16:26 UTC at 36.1°N, 140.1°E. The lidar data smoothed with a low-pass filter with a cutoff at 3 km is also plotted as a solid line (Professor Toshitaka Tsuda, Kyoto University, personal communication).

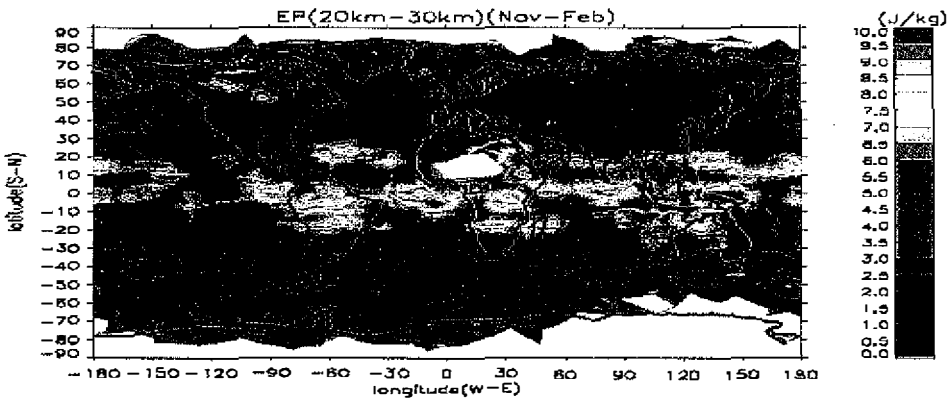


Fig. 13. Potential energy due to gravity waves computed from the 1996/97 GPS/MET temperature profiles (Tsuda et al., 2000).

COSMIC data can help improve analyses of surface air pressures in regions of low atmospheric water vapor. This is important to the GRACE (Gravity Recovery and Climate Experiment) mission. GRACE can detect the gravitational change due to changing ice sheets, if the

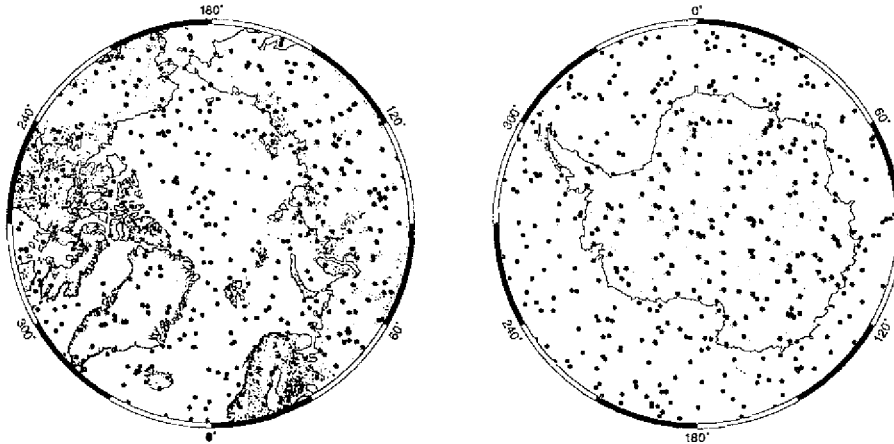


Fig. 14. Projected COSMIC soundings near the poles every 24 hours (green). Radiosonde sites are shown in red.

gravitational “noise” due to changing surface pressure (weight of the total column of air) is calibrated (Gurvich and Sokolovskiy, 1985). The data from COSMIC promise to improve this calibration and therefore the “ice signal” of GRACE. Additional studies, such as assimilation of simulated COSMIC refractivity observations into numerical weather models, are needed before we can state by how much pressure, temperature and moisture are improved near the surface. COSMIC data will also aid monitoring of atmospheric water vapor in the polar regions, an important parameter for mass balance studies of the ice sheets.

Weather analysis and forecasting in the polar regions are likely to be significantly enhanced by COSMIC and will have important applications in areas such as the aviation industry and in the execution of various scientific and commercial missions in these remote regions. To summarize some examples where COSMIC can be useful to polar meteorology:

- Improved meteorological analyses and forecasts
- Surface pressure corrections for ice balance studies with GRACE
- Vertical temperature profiles for ozone depletion studies
- Polar water vapor studies (assuming temperatures are known, or available through model assimilation of refractivity)
- Investigation of sudden stratospheric warming events during the polar spring
- Improved aviation weather analysis and prediction over the polar regions

### 3. COSMIC AND NUMERICAL WEATHER PREDICTION

COSMIC will generate meteorological products within three hours of observation for tests in operational weather prediction. This section expands upon the discussion of Anthes et al. (1997a) and argues that COSMIC data, if assimilated effectively in NWP models, will

improve global analyses and forecasts. This conclusion is supported by previous independent studies (Hoeg et al., 1996)

### 3.1 Effect on Analysis

Although the global coverage of data from the GPS/MET experiment was inadequate to make a difference operationally, the GPS/MET data did provide evidence that COSMIC data will have a significant positive impact on global operational analyses. For a new data set such as COSMIC to make a positive difference in an operational analysis and subsequent forecast, the data must add useful information by contributing differences to the analysis that make the analysis more accurate, especially in regions of the atmosphere that are sensitive to initial errors (Palmer et al., 1998). Leroy (1997) compared time-averaged analyses of geopotential heights computed from GPS/MET data with operational analyses over the same period from ECMWF and found large differences over data-sparse regions such as the South Pacific ocean. Since the differences were small over data-rich regions, this study suggests that COSMIC data will make a positive difference to operational analyses even at large scales over the oceans. Similarly, Rocken et al. (1997) found a significantly greater difference between GPS/MET refractivities and derived temperatures from NCEP analyses over data-poor regions versus data-rich regions (Fig. 15).

The four GPS/MET soundings shown in Fig. 11, taken during January and February 1997, show large differences in stratospheric temperatures observed by GPS/MET and the NCEP operational analyses. Since the soundings agree well in the lower troposphere, these systematic differences in the stratosphere suggest that the NCEP stratospheric analyses are biased toward temperatures that are too high and that COSMIC data will have a significant positive impact in the stratospheric analyses.

Further evidence that COSMIC data will significantly modify operational analyses is presented in Fig. 16, which shows comparisons for GPS/MET 100 mb temperatures over a 53-day period (January 6-February 27, 1997) with the NCEP/NCAR reanalysis (16a) and the ECMWF operational analysis (16b). Differences in GPS/MET temperatures and NCEP/NCAR temperatures range from - 5.8 K to + 3.4 K while the corresponding differences from the ECMWF analysis range from -3.3 to + 3.9 K. [Note that the color shading reflects an objective analysis of the temperature differences, which were calculated at the GPS/MET sounding sites (indicated in the figure by black dots). Temperature differences for individual soundings between GPS/MET and NCEP/NCAR temperature can be as large as 8 K.] The NCEP/NCAR temperatures show a systematic warm bias in the latitude band +/- 30 degrees from the Equator. This systematic warm bias is not present in the ECMWF analysis. Figure 16c shows the comparison of the ECMWF and NCEP/NCAR analyses over this period. The NCEP temperatures are higher than the ECMWF temperature over the Equator and lower between about 30°N and 60°N. The differences shown here are consistent with the temperature differences shown in the example in Fig. 10. These comparisons show that significant differences, and therefore uncertainties, exist between objective analyses from leading world meteorological centers. Hence COSMIC data can be expected to make a significant impact on operational analyses and re-analyses. Similar global comparisons will be conducted with COSMIC real-

time data and provided to operational centers as a tool for quality control and evaluation.

On smaller scales and over data-rich regions, it is difficult to estimate in advance what the impact of COSMIC data will be. However, the improved vertical resolution of upper-level fronts by GPS/MET soundings compared to the operational weather analyses, as illustrated in Figs. 6, 7 and 9, provide evidence that COSMIC data may have a positive impact on analyses even over data-rich regions. It is possible that the impact will be small on many days and large on a few significant days. Given the theoretical accuracy and high vertical resolution of COSMIC data, which have been confirmed by the GPS/MET experiment, and the data assimilation studies conducted so far (Kuo et al., 1997; 2000), we can reasonably expect a significant positive impact of COSMIC data on operational analyses.

### 3.2 Initialization of NWP Models Using COSMIC Data

COSMIC data will be available for testing in real-time in operational NWP models. It is likely that the data will be assimilated into the models using three-dimensional or four-dimensional variational techniques (3DVAR or 4DVAR). Either of these data assimilation techniques may, in principle, assimilate bending angles, refractivities, or derived temperature and water vapor data. Eyre (1994) suggests that the most powerful use of COSMIC neutral atmosphere data is to assimilate the refractivity or bending angle profiles directly into numerical models. In this way, which is analogous to assimilating satellite-observed radiances in models

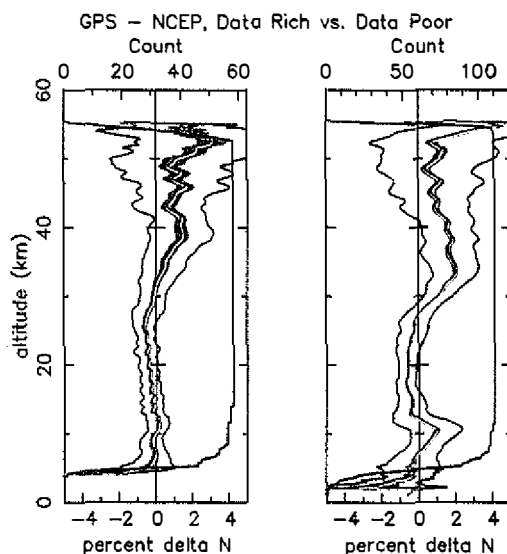


*Fig. 15.* GPS/MET minus NCEP refractivity profiles for data rich (left panel) and data poor (right panel) regions. Shown are the ensemble mean differences (red line), the standard deviation of the differences (black line), and the standard error of the mean differences (green envelope around red line). The blue line is the number of soundings at each level. (Rocken et al., 1997).

rather than soundings derived from these radiances (Derber and Wu, 1998), a minimum number of assumptions are made. Numerical experiments have shown that assimilation of refractivity and bending angles directly into numerical models causes the model's temperature, water vapor, and wind fields to adjust toward actual atmospheric values (Zou et al., 1995; Kuo et al., 1997, Zou et al., 1999). How this mutual adjustment occurs is investigated in the following sections.

### 3.2.1 Adjustment of Models to COSMIC Mass Field Data as Predicted by Geostrophic Adjustment Theory

COSMIC data will provide information on the temperature, pressure and water vapor fields of the atmosphere. These variables constitute the mass field of the atmosphere. For large scales of motion, the mass field is in near balance with the wind field, meaning that the

gps\_nmcrs\_temp\_100mb\_97.006-058

(a)

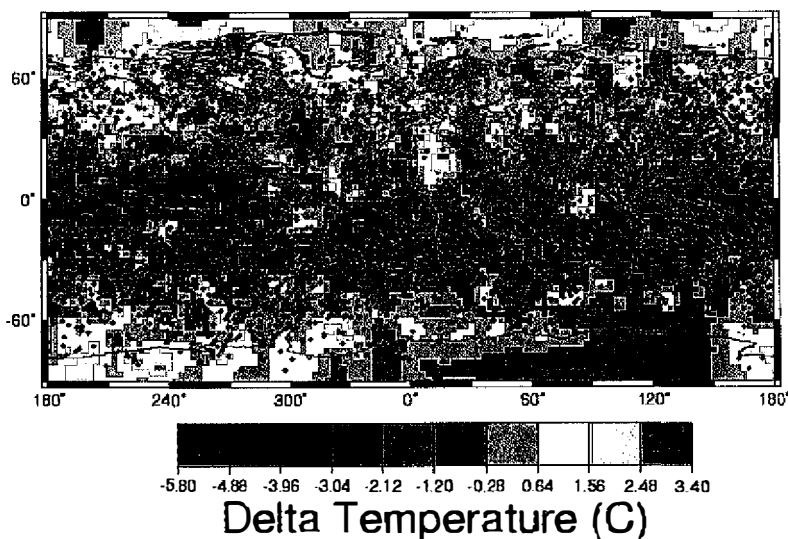
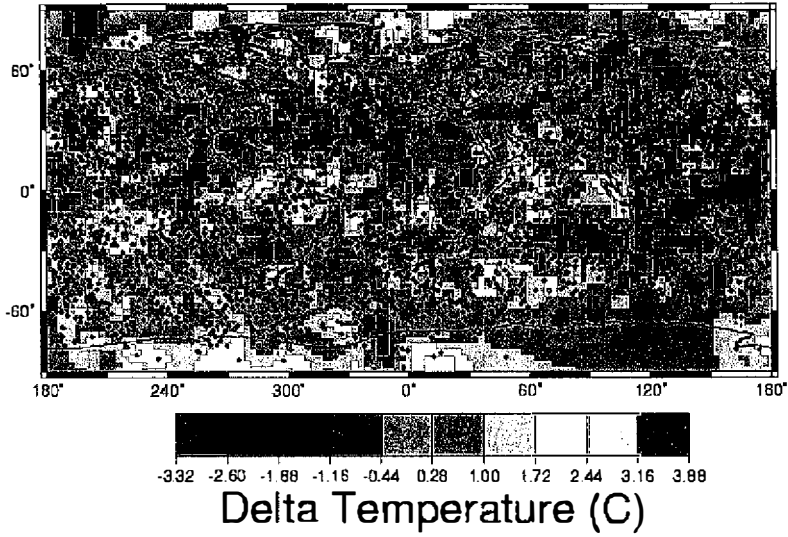


*Fig. 16.* GPS/MET minus analysis temperatures at 100 mb for (a) NCEP/NCAR reanalysis (Kalnay et al, 1996) and ECMWF(b). Note the difference in scale, and in the systematic differences in the equatorial regions between GPS/MET and NCEP. NCEP is significantly warmer than GPS/MET in the equatorial regions and somewhat cooler in middle latitudes. The systematic bias in the ECMWF analysis is much smaller. The difference map between the ECMWF and NCEP/NCAR temperatures at 100 mb shown in (c) indicate that significant differences, and hence uncertainties, exist even on large scales and over long time periods.

gps\_ecmwf\_temp\_100mb\_97.006-058

(b)



ecmwf\_nmcrs\_temp\_100mb\_97.006-058

(c)

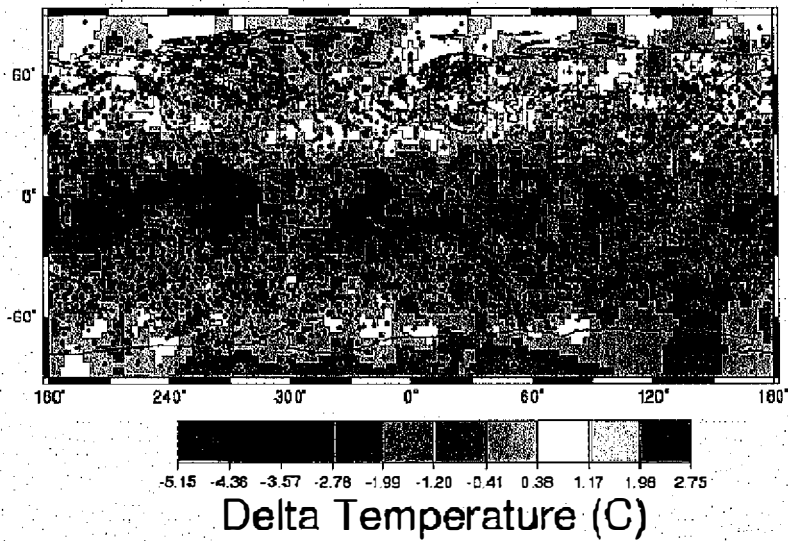


(Fig. 16. continued)

net accelerations of the wind are small compared to the accelerations associated with the Coriolis force and pressure gradient force individually. Under these conditions, accurate specification of either the three-dimensional mass field or the three-dimensional wind field determines the other through rather simple diagnostic relationships.

The type of balance between the mass and wind fields varies depending on the horizontal and vertical scales of motion of the atmospheric feature, the latitude, and whether or not significant acceleration effects are present. The important acceleration effects are associated with curved atmospheric flow, friction, and diabatic heating. The simplest balance is given by the geostrophic relationship in which the wind speed and direction are directly related to the horizontal pressure gradient force. Simple geostrophic balance is most valid for large-scale, straight flow in high latitudes in the absence of frictional or diabatic heating effects. Addition of curvature in the flow modifies the geostrophic wind relationship by accounting for centripetal acceleration effects; the result is the gradient wind relationship, which takes into account the radius of curvature of the trajectory. A further generalization for horizontal flow that takes into account nonlinear effects in the equation of motion results in the balance equation (Holton, 1979, p. 179).

In fact, the atmosphere is never in complete balance; it is continuously adjusting to small imbalances between the mass and the wind fields through the generation and propagation of inertial gravity waves.

For motion at small scales, low latitudes, or when friction or diabatic heating are present, the atmosphere often shows large departures from the balances described above and ageostrophic motions can be large. Under these conditions there are no simple diagnostic equations relating the wind and mass fields. However, through the data assimilation process, if one assimilates accurate observations of either the mass or the wind field into the model, the other field will adjust through the model's equations to an appropriate balance, even in the presence of these ageostrophic effects. Herein lies one of the great advantages of continuous data assimilation.

An important question is how will COSMIC data improve the initial conditions in NWP models and thereby improve the subsequent forecasts. COSMIC data provide independent and accurate information about the atmosphere's mass field. How will assimilation of these data affect the model's wind field? To help answer these questions, we consider geostrophic adjustment theory (see Haltiner and Williams, 1980, p.47 for an introduction to this theory).

Although, in principle, either mass or wind observations may be assimilated in models and the other field will adjust appropriately (Atlas et al., 1985), the efficiency of the adjustment process varies depending on the variable being assimilated, the horizontal and vertical scale of the phenomenon, the latitude, the static stability, and the nearness to the surface of the Earth. The relative efficiency of assimilating mass or wind observations may be investigated through geostrophic adjustment theory. In geostrophic adjustment theory, we assume that the atmosphere is in a quasi-balanced state but that small imbalances exist between the mass and the wind field. Since both the wind and the mass fields contain small errors, to assess the impact of COSMIC data on models, we ask how the model atmosphere will adjust to an input of accurate mass field data (data with an accuracy significantly above the accuracy of the model's mass field data).

To consider the relative importance of mass and wind observations in a model, consider a



linearized shallow fluid model on a resting basic state (Haltiner and Williams, 1980, p.48). This system consists of a steady state solution in geostrophic equilibrium and three wave solutions: two inertial gravity waves and a Rossby wave. If an imbalance between the mass and wind fields exists in the initial conditions, the system adjusts to the steady state geostrophic solution through the propagation of the inertial gravity waves away from the system. The final balanced state, denoted by subscript “s,” is related to the initial unbalanced state, denoted by subscript “o,” is given by the solution (Haltiner and Williams, 1980, p. 51)

$$V_s = \frac{1}{(1 + L_R^2/L^2)} \left( \frac{L_R^2}{L^2} V_o + i \frac{gh_o}{fL} \right), \quad (6)$$

and

$$h_s = \frac{1}{(1 + L_R^2/L^2)} \left( \frac{L_R^2}{L^2} \frac{fL}{ig} V_o + h_o \right), \quad (7)$$

where  $V_s(V_o)$  and  $h_s(h_o)$  represent the adjusted steady state (initial) wind and mass fields respectively,  $L$  is the wavelength of the perturbation,  $g$  is the acceleration of gravity,  $f$  is the Coriolis parameter,  $i = \sqrt{-1}$  and  $L_R$  is the Rossby radius of deformation given by

$$L_R = f^{-1}(gH)^{1/2}, \quad (8)$$

where  $H$  is the mean depth of the fluid.

Now, we assume that the Coriolis force and the pressure gradient force have the same order of magnitude, which means that  $V_o$  and  $\frac{gh_o}{fL}$  have the same order of magnitude. We get two very different final states depending on the scale of the disturbance. First consider the case where  $L^2 \ll L_R^2$ , in which case

$$V_s = V_o, \quad (6a)$$

and

$$h_s = \frac{fL}{ig} V_o. \quad (7a)$$

In this case, which is favored for small-scale horizontal disturbances with significant depth and low latitudes, the final wind is equal to the initial wind, and the final mass field is related geostrophically to the initial wind field. In this case the mass field has adjusted to the wind field, which means that accurate initial wind data would be more effective than accurate initial mass field data. Thus COSMIC data under these conditions would be relatively ineffective in causing the model wind field to adjust to the correct mass field data. The information in the COSMIC data will tend to radiate away as inertial gravity waves.

In the case where  $L^2 \gg L_R^2$ , a much different result is obtained. In this case (6) and (7) reduce to

$$V_s = \frac{igh_o}{fL}, \quad (6b)$$

and

$$h_s = h_o, \quad (7b)$$

Therefore, for large horizontal and shallow phenomena and high latitudes, the initial mass field determines the final state. Under these conditions, COSMIC data would be effective in causing the model's wind fields, as well as the mass fields, to adjust toward more accurate values.

As verified by more complex theories and by numerical experiments with non-linear models (Økland, 1970; Anthes, 1974; Hoke and Anthes, 1976; Hoke and Anthes, 1977), the above results are surprisingly general, applying to a two-dimensional barotropic atmosphere and to stably stratified baroclinic atmospheres. For the latter, the results apply if  $L_R = C_g / f$  where  $C_g$  is the phase speed of internal gravity waves

$$C_g = \frac{L_z}{2\pi} \left( \frac{g}{\theta} \frac{\partial \theta}{\partial z} \right)^{1/2}, \quad (9)$$

where  $\theta$  is potential temperature and  $L_z$  is the vertical scale of the phenomenon. Thus, in a stably stratified atmosphere, COSMIC observations will be most useful when the static stability is relatively low.

Table 3 shows values of the Rossby radius of deformation for some representative values of latitude, static stabilities and vertical scales of disturbance. This indicates that for the horizontal and vertical scales of motion resolved by the COSMIC data ( $L \geq 300$  km and  $L_z \geq 2$  km), the wind field will tend to adjust to the mass field, and COSMIC data will be effective in causing the model's wind fields to adjust. The situation where COSMIC data are least likely to be effective in this regard are for deep motions near the Equator under very stable conditions.

### 3.2.2 Data Assimilation and Geostrophic Adjustment

The classic theory of geostrophic adjustment as discussed above applies to the adjustment of a model atmosphere that is perturbed instantaneously by wind or mass field data. In a data assimilation cycle as practiced in modern operational centers, data are inserted into the model atmosphere more than once during an assimilation cycle; for example, data every six hours, or even every one hour, may be used in an assimilation cycle. For data derived from continuous observing systems such as satellites, the assimilation of data may occur nearly continuously over a 24-hour cycle. In this case, simple application of the geostrophic adjustment theory to interpret how the atmosphere adjusts to mass or wind data may be misleading. For example, consider a disturbance of a horizontal and vertical scale at a latitude in a model atmosphere with static stability such that for a given mass-field perturbation, half of the impulsive mass perturbation remains in the steady state adjusted wind field with the other half radiating away as inertial gravity waves. A second impulse of mass data a short time later would result in more than half of the mass field data being retained in the model's final wind field. And a continuous assimilation of accurate mass data would force the model's wind field to adjust to a value much closer to balance with the "final" mass field than would a single application of mass data.

The above argument suggests that even for short waves in tropical regions where geo-

strophic adjustment theory indicates that mass data will have less impact on the wind field, a continuous assimilation of mass data will have a much greater effect on the winds than simple geostrophic adjustment theory indicates. And in fact, data assimilation studies by Charney et al. (1969); Jastrow and Halem (1970, 1973), Williamson and Kasahara (1971), Kasahara (1972), Gordon et al. (1972) and others have shown that if any one of the three primary meteorological variables (wind, pressure or temperature) is assimilated over time in a model, the other two variables will adjust to the correct values (Atlas et al., 1985). Fig. 17 illustrates this fact by showing the reduction in wind error over time given the assimilation every 12 hours of temperature data with varying errors superimposed. In middle latitudes (49° in this example, 17a) the reduction in wind error is relatively rapid. At the Equator, the adjustment of the wind to the temperature data is slower in accordance with geostrophic adjustment theory, but even directly on the Equator there is a positive impact of assimilating accurate temperature data.

In another example, numerical experiments with a primitive equation model of a tropical cyclone indicate that continuous assimilation of accurate temperature data has almost as much positive effect on the model cyclone as does the continuous assimilation of both temperature and wind data (Fig. 18).

Near the Earth's surface, assimilation of temperature and pressure data has an advantage over assimilation of wind data. Small temperature changes in the free atmosphere as a result of insertion of accurate wind data occur through adiabatic cooling or warming associated with vertical motions resulting from imbalances between the adjusted wind field and the original mass field. Near the surface vertical motions are suppressed, and no amount of accurate wind data can correct an erroneous temperature field. Therefore, COSMIC data, which provide information on the temperature and pressure fields, will be particularly important in the lower kilometer or so of the atmosphere, and it is extremely important that a large fraction of COSMIC sounding reach to within one kilometer of the surface as planned.

In summary, we agree with the conclusions from the analysis of the value of GPS/MET soundings by Hoeg et al. (1996): "Atmospheric profiling using the radio occultation technique offer a major potential for improving the products from operational numerical weather

Table 3. Rossby Radius of Deformation ( $L_R$ ) for Vertical Scales of Phenomena Equal to 2 km and 5 km at Low, Middle and High Latitudes, and for Relatively Unstable and Stable Conditions.

For these calculations  $g=9.8\text{ms}^{-2}$  and  $\theta=330\text{K}$ .

Latitude	$L_z = 2 \text{ km}$		$L_z = 5 \text{ km}$	
	$\frac{\partial\theta}{\partial z} = 1 \text{ K/km}$	$\frac{\partial\theta}{\partial z} = 5 \text{ K/km}$	$\frac{\partial\theta}{\partial z} = 1 \text{ K/km}$	$\frac{\partial\theta}{\partial z} = 5 \text{ K/km}$
10°	69	153	171	383
40°	18	40	45	100
75°	12	28	31	69

prediction models. The observations from the technique will be one of the most economical ways of improving the observational data base for the NWP models. The good global data coverage will correct the forecast models by preserving the horizontal gradients in the atmospheric parameters.”

#### 4. COSMIC AND CLIMATE

Observing changes and variability in the global climate is one of the most important challenges in atmospheric sciences. Because of the many difficulties associated with making long-term in-situ measurements (for example calibration, representativeness, costs, difficulty in making temporally- continuous measurements over remote areas and throughout the entire troposphere and stratosphere), remote sensing from space is, in principle, the most desirable way to observe the global atmosphere over long periods of time. However, difficulties in obtaining reliable climate records from satellites include changes in instruments, platforms, Equator crossing times and algorithms (Hurrell and Trenberth, 1997, 1998; Salby and Callaghan, 1997; Waliser and Zhou, 1997). Calibration problems, instrument drift and lack of high vertical resolution add to the difficulties of observing small changes in climate or climate variability. The long-standing controversy associated with the Microwave Sounding Unit (MSU) is a case in point, as discussed by Hurrell and Trenberth (1998). The MSU tropospheric temperature record shows a slight global cooling (-0.05 K/decade) since 1979, whereas surface temperature records show a significant global warming (0.13 K/decade) over this same period. As noted by Hurrell and Trenberth, this discrepancy has been loudly touted by a few individuals as casting serious doubt on whether or not global warming is, in fact, occurring. The question about whether the global climate has warmed over the past several decades and by how much has thus become not only an important scientific question, but a political one as well.

The European Space Agency (ESA, 1996) describes many of the advantages and potential contributions of radio occultation data to climate studies. The recent National Research Council (NRC, 1998) assessment of the U.S. Global Change Research Program (USGCRP) emphasizes the importance of obtaining a long-term record of global temperature change that is accurate and stable. According to this report, “..an essential requirement of the observational strategy is to establish long-term, scientifically valid, consistent records for global change studies.” (NRC, 1998, p. 11). The NRC report also states (p. 26): “The importance of accuracy, continuity, calibration, documentation, and technological innovation in observations for long-term trend analysis of global change cannot be overemphasized.” The characteristics of the innovative radio occultation technique in general and COSMIC in particular include accuracy, long-term stability, no calibration, no instrument drift, unaffected by clouds, precipitation and aerosols and its high vertical resolution, all at relatively low cost. The technique is in many ways the ideal “global thermometer”, meeting many of the key objectives of the USGCRP as stated by the NRC and discussed recently by Goody et al. (1998).

The COSMIC mission will deliver data products that are unique and important for climate research. The special nature of GPS occultation data with regard to calibration is very crucial for detecting small variations and trends in climate, since data taken in different intervals by different research groups and from different countries can be compared without concern for

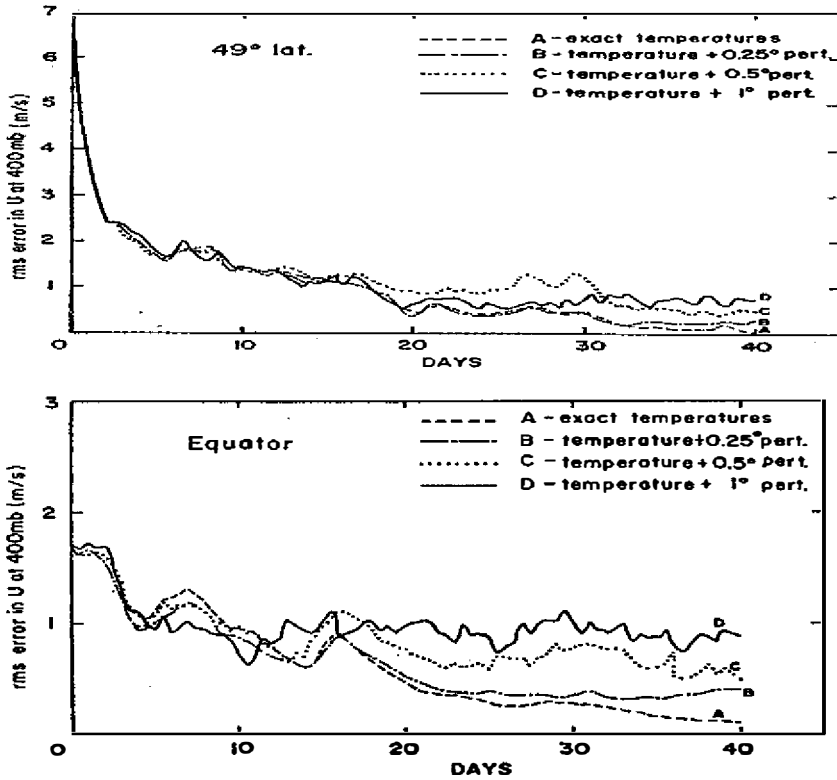


Fig. 17. Root-Mean-Square (RMS) error in the zonal wind (m/s) at 400 mb at (a) 49° latitude and (b) the Equator in cases where temperatures with random error perturbations of 0, 0.25, 0.5 and 1.0°C are inserted every 12 hours at all grid points. (Charney et al., 1969).

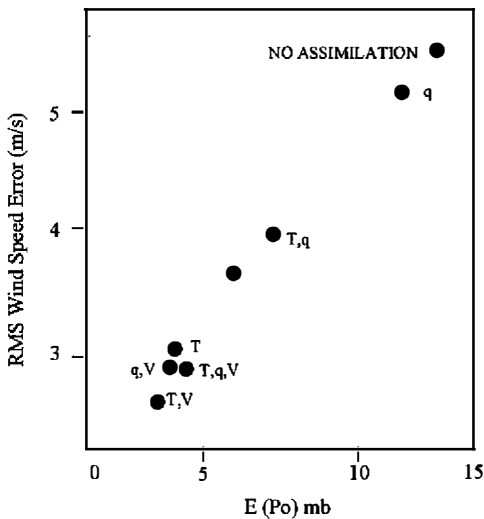


Fig. 18. Errors remaining in wind field and minimum pressure in a model tropical cyclone after 12 h of assimilating various combinations of wind (V), temperature (T), and specific humidity (q) data (Anthes, 1974).

instrument degradation or calibration. COSMIC will deliver 4,000 soundings/day with random measurement errors of about  $\pm 1$  K. For climate studies space-time averages of COSMIC observations can be formed to reduce the random error. A one-month average over each 1% area of the Earth's surface ( $\sim 1,200$  soundings) will reduce the random 1 K error to  $0.03^\circ\text{C}$ . This is adequate to follow trends of 0.1 K decade, which is typical of greenhouse gas or other forced climate responses. COSMIC data will provide seamless soundings from orbit altitude to near the surface. It has been shown (North and Stevens, 1998; Stevens, 1999; Leroy, 1998) that stratospheric-tropospheric temperature profile information enhances the signal-to-noise ratio of climate data significantly over surface-only observations. For example, Stevens (1998) showed that for a transient simulation of the doubling of carbon dioxide in the atmosphere, the signal-to-noise ratio for climate signal detection is increased by a factor of 2.3 when temperature data from the tropical upper troposphere and stratosphere are used, compared with using only the tropical surface temperature data. Over much of the Earth the greenhouse-warming signal in models is strongest in the upper troposphere and lower stratosphere (Fig. 19), where the accuracy of COSMIC data will be the highest.

The unique capability of COSMIC data in estimating the geopotential heights of constant pressure surfaces independent of surface pressure or temperature data can be used to monitor global or regional scale layer mean virtual temperature, which is a sensitive measure of global change. The mean virtual temperature  $T_v$  in an atmospheric layer from the surface ( $Z_s$ ) to the geopotential height of a constant pressure surface  $P_t$  is given by

$$T_v = \frac{g(Z_t - Z_s)}{R \ln \frac{P_s}{P_t}}, \quad (10)$$

where  $P_s$  is the surface pressure and  $R$  is the gas constant for dry air. Unlike other observing systems, COSMIC soundings can be used to calculate  $Z_t$  above the onset of water vapor independent of any data below this height by integrating the hydrostatic equation downward from great heights to any pressure level. Changes over time of  $Z_t$  are thus proportional to the changes in mean virtual temperature in the atmospheric layer from  $Z_t$  to the Earth's surface, and thus provide an integral measure of global change through deep layers of the atmosphere.

According to model studies, and suggested by observations over the past 25 years (IPCC, 1996) the lower tropospheric vapor concentrations will increase with increasing surface temperature (the water-vapor feedback effect). The situation is not so clear in the upper troposphere, where small amounts of water vapor are important for radiative heat transfer. Lindzen (1990) argues that increased surface temperature and resulting stronger tropical convection will result in increased tropical precipitation and a decrease of tropical/subtropical tropospheric moisture above 6 km. This is in contrast to model predictions of water vapor increases of 20% per degree of surface warming. Clearly it is important to resolve the differing theories and to test the performance of climate models in simulating upper troposphere water vapor. This, however, may be difficult with current observing systems as Rind (1998) points out. Radiosondes are not suitable for detecting long-term global trends, and down-looking radiometers lack the required vertical resolution. COSMIC data will help the situation. Assuming that temperature is known at the 500 mb level from models to within 1-2 degrees, individual

COSMIC profiles will measure the water vapor pressure at that height to about 0.2 mb, or, assuming all errors are random, averaged over a 1% 1-month 1,200-sounding "climate box", to 0.006 mb. Water vapor pressure at 500-mb height varies between 0 - 6 mb and a several percent change, especially in the tropics, should be detectable by COSMIC data with high vertical resolution. At 300 mb GPS/MET observed water vapor in the range 0-0.7 mb. Following the same arguments as above, water vapor at that altitude can be measured to  $\sim 0.12$  mb, or to a climatological average of 0.004 mb.

Figure 20 shows GPS/MET derived water vapor (using ECMWF temperatures) at 300 and 500 mb for two different time windows. These results have not been validated with correlative data but look generally reasonable with the highest amounts over regions of deep convection. The East Asian monsoon shows up clearly during the June-July period, and we see the high water vapor values over Africa and South America, presumably caused by convection.

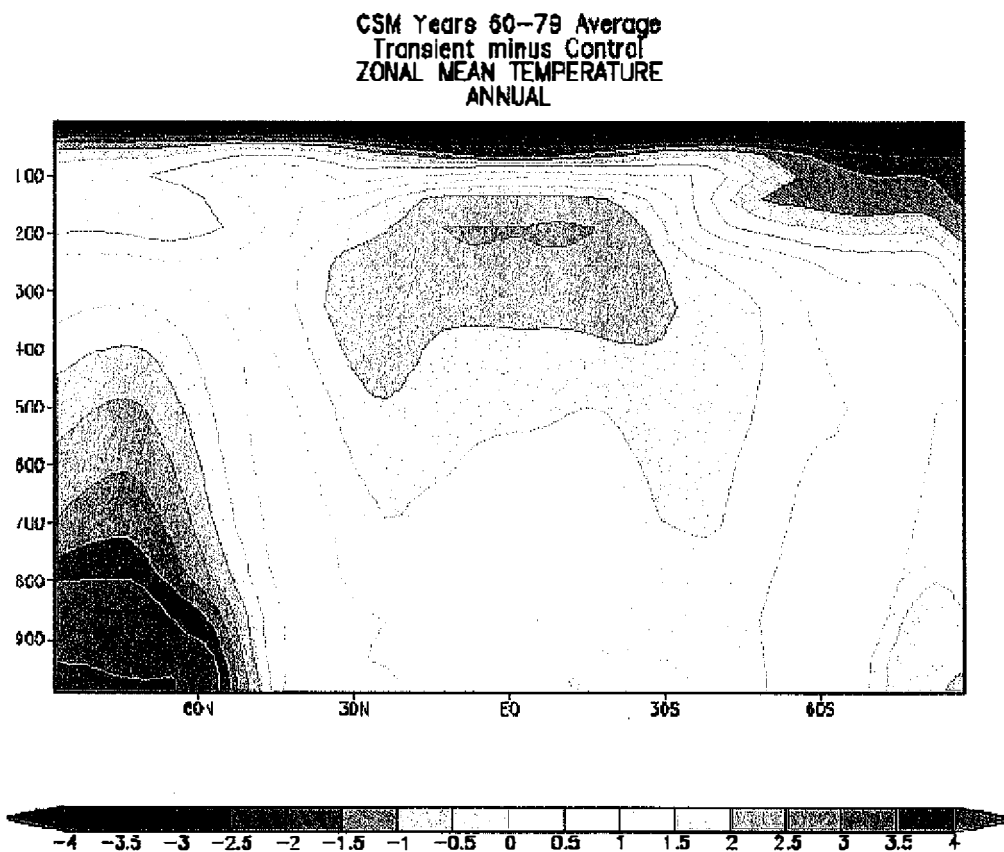


Fig. 19. Vertical cross sections of zonally-averaged model temperature changes averaged over 20 years (years 60-79) in NCAR Climate System Model in which carbon dioxide alone is increased by 1% per year (Meehl et al., 2000).

While each panel in Fig. 20 represents 15 or 22 days of data, COSMIC will provide a similar view of the global atmosphere (there are about 1000 occultation soundings in each panel) every six hours. Thus COSMIC will contribute to our understanding of the global hydrologic cycle, which is the goal of GEWEX (Global Energy and Water Cycle Experiment) GVaP (GEWEX Water Vapor Project) (Chahine, 1997; Anthes et al., 1997b).

Because of its insensitivity to smoke and aerosols, COSMIC data will also be useful in studying the effect of volcanoes or large fires on climate and related global change studies. The Mt. Pinatubo eruption in 1991 caused significant changes in the global climate with warming in the stratosphere of up to 1 K and cooling in the troposphere of more than 1 K in certain regions (Fiocco et al., 1996). Both the stratospheric warming and tropospheric cooling patterns showed large variations in space—patterns that could be resolved with COSMIC data. Christopher et al. (1998) show that the biomass burning in South America significantly perturbs the regional climate. The Kuwait oil fires of 1991 (Husain, 1995) perturbed the weather and short-term climates of this region significantly. Accurate, high-resolution global measurements over a long period of time are usually difficult to obtain because the events often occur in remote regions, and the environment is hostile to making in-situ measurements. COSMIC can contribute to studies of perturbations to climate by similar episodic events.

Key scientific contributions of COSMIC to climate research are listed below.

- Provide a global self-calibrating data set for climate monitoring and climate model testing
- Monitor water vapor distribution, especially in the tropics
- Study troposphere/stratosphere exchange
- Study the effects of volcanic eruptions and large fires on climate
- Stimulate development of new climate change parameters (i.e. profiles of bending angles)
- Stimulate new climate statistics and correlation studies

## 5. SUMMARY

This paper has reviewed the characteristics of the COSMIC data set and some of the ways that they can be used in meteorological research and operational weather prediction and climate monitoring and research. COSMIC data offer a number of unique advantages that complement existing research and operational observing systems and, together with these systems, offer the potential to improve understanding of global and regional atmospheric processes and to improve weather forecasts and climate projections into the future. Table 4 summarizes the most important scientific contributions to atmospheric science, including meteorology and climate, that COSMIC will provide.

The characteristics and wide range of applications as summarized in Table 4 and in this paper will contribute significantly to a number of national and international programs. These include, for example, the U.S. Global Change Research Program, the U.S. Weather Research Program, the World Weather Research Program, the Atmospheric Radiation Measurements (ARM) program, and the World Climate Research Programme and its projects (GEWEX),



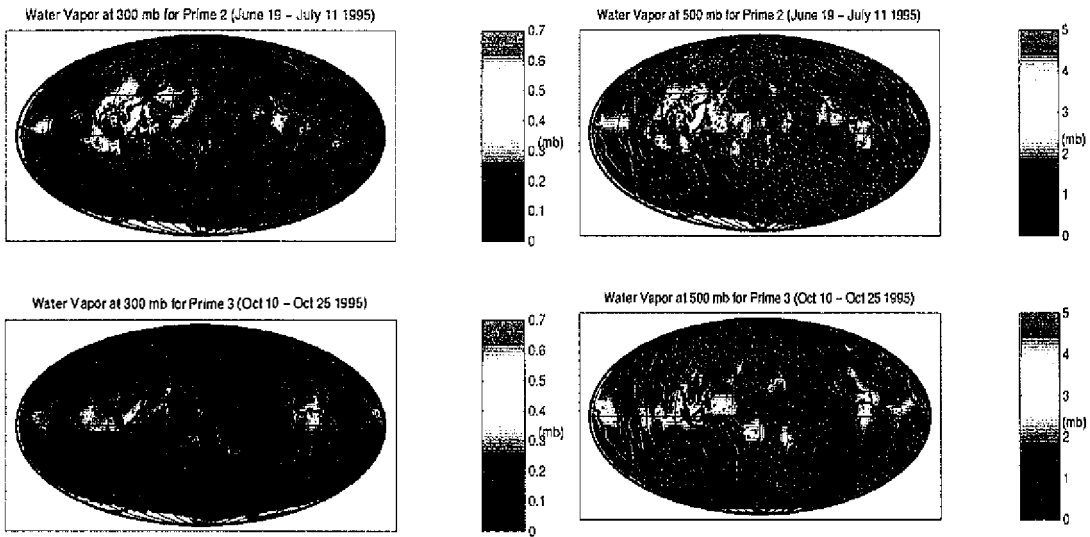


*Fig. 20.* Middle (500 mb) and upper (300 mb) tropospheric water vapor for period June 19 through July 11, 1995 and October 10-25, 1995 computed from GPS/MET refractivity data and ECMWF temperature data. Occultation locations are shown by black dots.

Stratospheric Processes and their role in Climate (SPARC), Climate Variability and Predictability study (CLIVAR), Arctic Climate System Study (ACSYS), and the World Ocean Circulation Experiment (WOCE). COSMIC will also contribute to the International Geosphere-Biosphere Programme (IGBP) in the effort to develop an understanding and ability to model and ultimately predict the evolution of the fully-coupled Earth system. Finally, COSMIC data will support the scientific assessments of the Intergovernmental Panel on Climate Change (IPCC, 1996).

**Acknowledgments** The authors acknowledge the support of the National Science Foundation for the GPS/MET proof-of-concept experiment and for the leadership role played by NSF, particularly Drs. Jay Fein, Dick Greenfield and Bob Corell in the development of the COSMIC experiment. Doug Hunt provided invaluable assistance in processing the GPS/MET data used in this study. Susan Montgomery-Hodge and Susie Siders provided expert assistance in preparing this manuscript. UCAR has been funded by Taiwan's National Space Program Office (NSPO) for developing the COSMIC system and concepts. Finally, we acknowledge Drs. Ching-Yen Tsay (Vice-Chairman of the National Science Council in Taiwan), Chao-Han Liu (President of National Central University in Taiwan), Dr. Hung-Chih Wang (Director of NSPO), and Dr. David Chu (NSPO) for their leadership and support of COSMIC.

Table 4. Applications of COSMIC data to atmospheric sciences, including weather and climate research and operational weather prediction.

<ul style="list-style-type: none"> <li>• Provide 4000 accurate soundings per day globally and in all weather with high vertical resolution of bending angle, refractivity and derived products such as temperature and water vapor in stratosphere and troposphere.</li> </ul>
<ul style="list-style-type: none"> <li>• Calculate temperature directly where water vapor is negligible (e.g. stratosphere, upper troposphere).</li> </ul>
<ul style="list-style-type: none"> <li>• Calculate water vapor directly where temperature is fairly well known independently.</li> </ul>
<ul style="list-style-type: none"> <li>• Estimation of winds through geostrophic or gradient wind relationships in high latitudes or through assimilation of data in models.</li> </ul>
<ul style="list-style-type: none"> <li>• Direct assimilation of bending angle or refractivity in numerical models to recover temperature, water vapor and winds.</li> </ul>
<ul style="list-style-type: none"> <li>• Improve global analyses in real time and research mode (e.g. reanalysis) to obtain improved estimates of temperature, water vapor and winds, particularly over oceans and polar regions.</li> </ul>
<ul style="list-style-type: none"> <li>• Improve vertical resolution of upper-level fronts and associated jet streams and tropopause, supporting process studies such as tropospheric-stratospheric exchange.</li> </ul>
<ul style="list-style-type: none"> <li>• Improve understanding of global water cycle, climatology of water vapor.</li> </ul>
<ul style="list-style-type: none"> <li>• Investigation of gravity waves in the stratosphere.</li> </ul>
<ul style="list-style-type: none"> <li>• Investigation of effects of large fires and volcanoes on weather and climate.</li> </ul>
<ul style="list-style-type: none"> <li>• Resolve the diurnal cycle of temperature globally</li> </ul>
<ul style="list-style-type: none"> <li>• Monitor global and regional temperature change with unprecedented accuracy, vertical resolution and stability in troposphere and stratosphere for climate and global change studies.</li> </ul>
<ul style="list-style-type: none"> <li>• Resolve discrepancies in temperature records from various sources (e.g. the Microwave Sounder Unit inferred temperature record compared to surface temperature record measured by in-situ instruments).</li> </ul>
<ul style="list-style-type: none"> <li>• Monitor global distribution of geopotential heights for climate and global change studies.</li> </ul>
<ul style="list-style-type: none"> <li>• Introduce bending angle and refractivity as new climate change parameters.</li> </ul>
<ul style="list-style-type: none"> <li>• Stratospheric studies, including ozone depletion, stratospheric-tropospheric exchange and volcanic effects.</li> </ul>
<ul style="list-style-type: none"> <li>• Improve global and regional numerical weather predictions and operational forecasts.</li> </ul>
<ul style="list-style-type: none"> <li>• Complement existing observing systems and provide independent data for development of improved analysis systems using merged observations.</li> </ul>
<ul style="list-style-type: none"> <li>• Provide data to calibrate or interpret other satellite-based sounding systems on GOES, POES and EOS.</li> </ul>
<ul style="list-style-type: none"> <li>• Provide data to support research field programs (e.g. programs like TOGA-COARE, INDOEX, JASMINE, FASTEX).</li> </ul>

## REFERENCES

- Anthes, R. A., 1974: Data assimilation and initialization of hurricane prediction models. *J. Atmos. Sci.*, **31**, 702-719.
- Anthes, R. A., 1982: Tropical cyclones-Their evolution, structure and effects, Meteorological Monographs. 19, No. 41, American Meteorological Society, Boston, 208 pp.
- Anthes, R., W. Schreiner, S. M. Exner, D. Hunt, Y. Kuo, Sokolovskiy, R. Ware and X. Zou, 1997a: GPS Sounding of the Atmosphere from Low Earth Orbit: Preliminary Results and Potential Impact on Numerical Weather Prediction, Augmenting the GPS Infrastructure for Earth, GPS for the Geosciences, National Academy Press, 114-124.
- Anthes, R., M. Exner, C. Rocken, and R. Ware, 1997b: Results from the GPS/MET Experiment and Potential Applications to GEWEX, *GEWEX News*, **7**, 3-6.
- Atlas, R., E. Kalnay, and M. Halem, 1985: Impact of satellite temperature sounding and wind data on numerical weather prediction. *Optical Engineering*, **24**, 341-346.
- Bevis, M., S. Businger, T. A. Herring, C. Rocken, R. A. Anthes, and R. H. Ware, 1992: GPS Meteorology: Remote Sensing of Atmospheric Water Vapor using the Global Positioning System. *J. Geophys. Res.*, **97**, 15,787-15,801.
- Belloul, B., and A. Hauchecorne, 1997: Effect of periodic horizontal gradients on the retrieval of atmospheric profiles from occultation measurement. *Radio Science*, **32**, 469-478.
- Businger, S., S. Chiswell, M. Bevis, J. Duan, R. Anthes, C. Rocken, R. Ware, M. Exner, T. VanHove, and F. Solheim, 1996: The Promise of GPS in Atmospheric Monitoring. *Bull. Amer. Met. Soc.*, **77**, 5-18.
- Chahine, M., 1997: The future direction of the GEWEX Global Water Vapor Project (GvaP). *GEWEX News*, **7**, p.2.
- Charney, J., M. Halem, and R. Jastrow, 1969: Use of incomplete historical data to infer the present state of the atmosphere. *J. Atmos. Sci.*, **26**, 1160-63.
- Christopher, S.A., M. Wang, J.A. Berender, R.M. Welch, and S.-K. Yang, 1998: The 1985 biomass burning season in South America: Satellite remote sensing of fires, smoke and regional radiative energy budgets. *J. Appl. Met.*, **37**, 661-668.
- Davis, C.A., and K.A. Emanuel, 1991: Potential vorticity diagnostic of cyclogenesis. *Mon. Wea. Rev.*, **119**, 1929-1953.
- Derber, J. C., and W. -S. Wu, 1998: The use of TOVS cloud-cleared radiances in the NCEP SSI analysis system. *Mon. Wea. Rev.*, **126**, 2287-2302.
- Duck, J., J. A. Whiteway, A. I. Carswell, 1998: Lidar observations of gravity wave activity and Arctic stratospheric vortex core warming. *Geophys. Res. Letters*, **25**, No. 15, 2813-2816.
- ESA, 1996: Atmospheric Profiling Mission. ESA SP-1196(7). The Nine Candidate Earth Explorer Missions. European Space Agency, ESA Publications Division, Noordwijk, The Netherlands, 58 pp.
- Eyre, J., 1994: Assimilation of radio occultation measurements into a numerical weather prediction system, Tech. Memo.199, Eur. Cent. For Medium Range Weather Forecasts, Reading, England.

- Fehlmann, R., and H. C. Davies, 1997: Misforecasts of synoptic systems: Diagnosis via PV Retrodiction. *Mon. Wea. Rev.*, **125**, 2247-2264.
- Fiocco, G., D. Fua, and G. Visconti, 1996: The Mount Pinatubo eruption: Effects on the atmosphere and climate. Springer, New York, 310 pp.
- Gelaro, R., R. Buizza, T. N. Palmer, and E. Klinker, 1998: Sensitivity analysis of forecast errors and the construction of optimal perturbations using singular vectors. *J. Atmos. Sci.*, **55**, 1012-1037.
- Goody, R., J. Anderson, and G. North, 1998: Testing climate models: An approach. *Bull. Amer. Met. Soc.*, **79**, 2541-2549.
- Gorbunov, M.E., and A.S. Gurvich, 1998: Microlab-1 experiment: Multipath effects in the lower troposphere. *J. Geophysical Res.*, **103**, 13819-13826.
- Gorbunov, M.E., S. V. Sokolovskiy, and L. Bengtsson, 1996a: Space refractive tomography of the atmosphere: modeling of direct and inverse problem. Rep. No. 210, Max Planck Inst. for Meteorology, Hamburg, 59 pp.
- Gorbunov, M.E., A.S. Gurvich, and L. Bengtsson, 1996b: Advanced algorithms of inversion of GPS/MET satellite data and their applications to reconstruction of temperature and humidity, Rep. 211, Max Planck Inst. For Meteorology, Hamburg.
- Gordon, C.T., L. Umscheid, Jr., and K. Miyakoda, 1972: Simulation experiments for determining wind data requirements in the tropics. *J. Atmos. Sci.*, **29**, 1064-75.
- Gurvich, A. S., and S. V. Sokolovskiy, 1985: Reconstruction of a pressure field by remote refractometry from space, *Izvestiya. Atm. Ocean. Phys.*, **21**, 7-13.
- Hajj, G. A., and L. J. Romans, 1998: Ionospheric electron density profiles obtained with the GPS: Results from the GPS/MET experiment. *Radio Science*, 33, No. 1, pp. 175-190.
- Haltiner, G. J., and R. T. Williams, 1980: Numerical Prediction and Dynamic Meteorology Second Edition, Wiley, New York, 477 pp.
- Hocke K., 1997: Inversion of GPS meteorology data. *Ann. Geophys.*, **15**, 443-450.
- Hoeg, P., A. Hauchecorne, G. Kirchengast, S. Syndergaard, B. Belloul, R. Leitingner, and W. Rothleitner, 1996: Derivation of atmospheric properties using a radio occultation technique, *Sci. Rep.*, 95-4, Danish Meteorol. Inst.
- Hoke, J. E., and R. A. Anthes, 1976: The initialization of numerical models by a dynamic-initialization technique. *Mon. Wea. Rev.*, **104**, 1551-1556.
- Hoke, J. E., and R. A. Anthes, 1977: Dynamic initialization of a three-dimensional primitive-equation model of Hurricane Alma of 1962. *Mon. Wea. Rev.*, **105**, 1266-1280.
- Holton, J. R., 1979: An Introduction to Dynamic Meteorology, Second Edition. Academic Press, New York, 391 pp.
- Hurrell, J. W., and K. E. Trenberth, 13 March 1997: Spurious trends in satellite MSU temperature from merging different satellite records. *Nature*, 386.
- Hurrell, James W., and Kevin E. Trenberth, 1998: Difficulties in obtaining reliable temperature trends: Reconciling the surface and satellite microwave sounding unit records. *J. Climate*, **11**, No. 5, pp. 945-967.
- Husain, T., 1995: Kuwaiti oil fires: Regional environmental perspectives. 1<sup>st</sup> Ed. Pergamon, Oxford, NY.
- IPCC, 1996: Climate change 1995. The science of climate change. Contribution of WGI to

- the second assessment report of the Intergovernmental Panel on Climate Change. Cambridge University Press, Cambridge, UK, 572 pp.
- Jastrow, R., and M. Halem, 1970: Simulation studies related to GARP. *Bull. Amer. Met. Soc.*, **51**, 490-513.
- Jastrow, R., and M. Halem, 1973: Simulation studies and design of First GARP Global Experiment. *Bull. Amer. Met. Soc.*, **54**, 13-21.
- Kalnay, E., M. Kanamitsu, R. Kistler, W. Collins, D. Deaven, L. Gandin, M. Iredell, S. Saha, G. White, J. Woollen, Y. Zhu, M. Chelliah, W. Ebisuzaki, W. Higgins, J. Janowiak, K. C. Mo, C. Ropelewski, J. Wang, A. Leetmaa, R. Reynolds, R. Jenne, and D. Joseph, 1996: The NCEP/NCAR 40-year reanalysis project. *Bull. Amer. Met. Soc.*, **77**, 437-471.
- Kasahara, A., 1972: Simulation experiments for meteorological observing systems for GARP. *Bull. Amer. Met. Soc.*, **53**, 252-264.
- Kuo, Y.-H., X. Zou, and W. Huang, 1997: The impact of GPS data on the prediction of an extratropical cyclone: An observing system simulation experiment. *J. Dyn. Atmos. Ocean*, **27**, 439-470.
- Kuo, Y.-H., X. Zou, S.-J. Chen, Y.-R. Guo, W. Huang, R. Anthes, D. Hunt, M. Exner, C. Rocken, and S. Sokolovskiy, 1998: A GPS/MET sounding through an intense upper-level front. *Bull. Amer. Met. Soc.*, **79**, 617-626.
- Kuo, Y.-H., S. Sokolovskiy, R. A. Anthes, and F. Vandenberghe, 2000: Assimilation of GPS Radio Occultation Data for Numerical Weather Prediction. *TAO*, **11**, 157-186.
- Kursinski, E. R., G. A. Hajj, W. I. Bertiger, S. S. Leroy, T. K. Meehan, L. J. Romans, J. T. Schofield, D. J. McCleese, W. G. Melbourne, C. L. Thornton, T. P. Yunck, J. R. Eyre, and R. N. Nagatani, 1996: Initial results of radio occultation observations of Earth's atmosphere using the Global Positioning System. *Science*, **271**, 1107-1110.
- Kursinski, E. R., G. A. Hajj, J. T. Schofield, R. P. Linfield and K. R. Hardy, 20 Oct. 1997: Observing the Earth's atmosphere with radio occultation measurements using the Global Positioning System. *J. Geophys. Res.*, **102**, No. D19, pp 23429-23465.
- Kursinski et al., 2000: The GPS radio occultation technique. *TAO*, **11**, 53-114.
- Lemoine, F.G., C. Kenyon, J. K. Factor, R. G. Trimmer, N. K. Pavlis, D. S. Cinn, C. M. Cox, S. M. Klosko, S. B. Iuthke, M. H. Torrence, Y. M. Wang, R. G. Williamson, E. C. Pavlis, R. H. Rapp, and T. R. Olsen, 1998: The development of the joint NASA GSFC and the National Imagery and Mapping Agency (NIMA) Geopotential Model EGM96, NASA/TP-1998-206861.
- Leroy, S., 1997: The measurement of geopotential heights by GPS radio occultation. *J. Geophys. Res.*, **102**, 6971-6986.
- Leroy, S. S., 1999: Optimal detection of global warming using temperature profiles: A methodology. *J. Climate*, **12**, 1185-1198.
- Lindzen, R. S., and M. Fox-Rabinovitz, 1989: Consistent vertical and horizontal resolution. *Mon. Wea. Rev.*, **117**, 2575-2583.
- Lindzen, R. S. 1990: Some coolness concerning global warming. *Bull. Amer. Met. Soc.* **71**, 288.
- Meehl, G. A., W. Collins, B. Boville, J. T. Kiehl, T. M. L Wigley, and J. M. Arblaster, 2000:

- Response of the NCAR Climate System Model to increased CO<sub>2</sub> and the role of physical processes. *J. Climate*, (in press).
- Melbourne, W., E. Davis, C. Duncan, G. Hajj, K. Hardy, E. Kursinski, T. Meehan, L. Young, and T. Yunck, 1994: The application of space borne GPS to atmospheric limb sounding and global change monitoring. *JPL Publ.*, 94-18, 147 pp.
- Menzel, W. P., F. C. Holt, T.J. Schmit, R.M. Aune, A. J. Schreiner, G.S. Wade, and D.G. Gray, 1998: Application of GOES-8/9 soundings to weather forecasting and nowcasting. *Bull. Amer. Met. Soc.*, **79**, 2059-2077.
- North, G. R., and M. J. Stevens, 1998: Detecting climate signals in the surface temperature record. *J. Climate*, **11**, 563-577.
- NRC, 1998: Global environmental change-Research pathways for the next decade. National Academy Press, Washington, D.C., 69 pp.
- Økland, H., 1970: On the adjustment toward balance in primitive equation weather prediction models. *Mon. Wea. Rev.*, **98**, 271-279.
- Palmer, T. N., R. Gelaro, J. Barkmeijer, and R. Buizza, 1998: Singular vectors, metrics and adaptive observations. *J. Atmos. Sci.*, **55**, 633-653.
- Pielke, R. A. Jr., and R. A. Pielke Sr., 1997: Hurricanes-Their nature and impacts on society. Wiley, New York, 279 pp.
- Rind, D., 1998: Just add water vapor. *Science*, **281**, 1152.
- Rocken, C. R. H. Ware, T. Van Hove, F. Solheim, C. Alber, J. Johnson, M. Bevis, and S. Businger, Dec. 1993: Sensing atmospheric water vapor with the Global Positioning System. *Geophys. Res. Letters*, **20**, 2631-2634.
- Rocken, C., T. Van Hove, J. Johnson, F. Solheim, R. Ware, M. Bevis, S. Businger, and S. Chiswell, 1995: GPS Storm - GPS sensing of atmospheric water vapor for meteorology. *J. Oceanic and Atmos. Tech.*, **12**, 468-478.
- Rocken, C., R. Anthes, M. Exner, D. Hunt, S. Sokolovskiy, R. Ware, M. Gorbunov, W. Schreiner, D. Feng, B. Herman, Y. Kuo, and X. Zou, 1997: Analysis and validation of GPS/MET data in the neutral atmosphere. *J. Geophys. Res.*, **102**, 29849-29866.
- Rocken, C., Y.-H. Kuo, W. Schreiner, D. Hunt, and S. Sokolovskiy, 2000: COSMIC system description. *TAO*, **11**, 21-52.
- Salby, M. L., and P. Callaghan; 1997: Sampling error in climate properties derived from satellite measurements: Consequences of undersampled diurnal variability. *J. Climate*, **10**, 18-36.
- Schoeberl, M. R., and D. L. Hartmann, 1991: The Dynamics of the stratospheric polar vortex and its relation to springtime ozone depletion. *Science*, **251**, 46-52.
- Schreiner, W. S., S. Sokolovskiy, C. Rocken, and D. C. Hunt, 1999: Analysis and validation of GPS/MET radio occultation data in the ionosphere. *Radio Science*, **34**, No. 41, 949-966.
- Staley, D. O., and R. L. Gall, 1977: On the wavelength of maximum baroclinic instability. *J. Atmos. Sci.*, **34**, 1679-1688.
- Stevens, M. J., 1999: Optimal climate signal detection in four dimensions. *JGR-Atmospheres*, **104**, D4, 4089-4099.

- Solheim, F. S., J. Vivekanandan, R. Ware, and C. Rocken, 1999: Propagation delays induced by dry air, water vapor, hydrometeors and other particulates. *JGR-Atmospheres*, **104**, D8, 9663-9670.
- Tsuda, T., Nishida N., Rocken C., and R. Ware, 2000: A global morphology of gravity wave activity in the stratosphere revealed by the GPS occultation data (GPS/MET), *JGR-Atmospheres*, 105 (in press).
- Waliser, D. E., and W. Zhou, 1997: Removing satellite equatorial crossing time biases from the OLR and HRC data sets. *J. Climate*, **10**, 2125-2146.
- Ware, R., 1992: GPS sounding of Earth's atmosphere. *GPS World*, **3**, 56- 57.
- Ware, R., M. Exner, D. Feng, M. Gorbunov, K. Hardy, B. Herman, Y. Kuo, T. Meehan, W. Melbourne, C. Rocken, W. Schreiner, S. Sokolovskiy, F. Solheim, X. Zou, R. Anthes, S. Businger, and K. Trenberth, 1996: GPS sounding of the atmosphere from low Earth orbit: Preliminary results. *Bull. Amer. Met. Soc.*, **77**, 19-40.
- WCRP, 1998: Stratospheric Processes and Their Role in Climate. World Climate Research Programme Report 105, World Meteorological Organization, Geneva, 131 pp.
- Williamson, D., and A. Kasahara, 1971: Adaptation of meteorological variables forced by updating. *J. Atmos. Sci.*, **28**, 1313-1324.
- Zou, X., Y.-H. Kuo, and Y.-R. Guo, 1995: Assimilation of atmospheric radio refractivity using a nonhydrostatic mesoscale model. *Mon. Wea. Rev.*, **123**, 2229-2249.
- Zou, X., F. Vandenberghe, B. Wang, M. E. Gorbunov, Y.-H. Kuo, S. Sokolovskiy, J.C. Chang, J. G. Sela, and R. A. Anthes, 1999: A ray-tracing operator and its adjoint for the use of GPS/MET refraction angle measurements. *JGR-Atmospheres*, **104**, D18, 22301-22318.

## APPENDIX A

### Spatial Resolution of Atmospheric Features by Radio Occultation Data

To obtain insights into how COSMIC data will contribute to the resolution (defined here as the ability to define or analyze) atmospheric features of various horizontal and vertical spatial scales, we must consider both the vertical and horizontal scales represented by an individual occultation sounding observation ("data point") and the vertical and horizontal data densities (defined by the average distance separating observations in space) of the set of observations. The spatial resolution, as defined above, of any observing system must consider both characteristics of the system.

We first consider the spatial scale, or spatial representativeness, of a single radio occultation observation (which in its raw form is the bending angle of a single ray). An observation of an atmospheric variable such as refractivity represents a weighted average of atmospheric properties over a volume represented by a near-horizontal tube (Fig. 1). This volume has an along-track length scale of approximately 300 km and a diameter of order 1 km. The horizontal or vertical scale of this observation is a measure of the horizontal or vertical distance over which the atmosphere contributes most of the information to the numerical value of the observation. The observation is often defined at a point (e.g. for comparison with other observa-

tions such as radiosonde data), but in reality contains contributions from the atmosphere enclosed by the tubular volume surrounding that point. Thus the scale may also be interpreted as the scale of the smearing of the true point-value observational variable. Fig. 2 shows a typical along-track weighting function that quantifies the relative contributions to the observation value, defined at  $x=0$ , from the atmosphere at distances away from  $x=0$ .

More precisely, we may define the vertical scale  $Z$  as the vertical distance perpendicular to the ray tangent that defines the layer of depth  $Z$  that contributes some fraction (e.g. 50%) to the value of the observation. Similarly, the horizontal scale of an occultation sounding may be defined as the horizontal distance along the track of the ray (along-track scale) or normal to the track (cross-track scale) that contributes 50% of the information to the derived refractivity. According to this definition, the horizontal scale associated with the weighting function graphed in Fig. 2 is approximately 300 km.

In contrast to horizontal or vertical scale associated with a single observation, the horizontal data density is defined as the average spacing between soundings obtained in a fixed period of time (e.g. a day). The horizontal data density is determined by the number and distribution of global soundings for the period. The vertical data density is defined as the average vertical distance between individual data points in the sounding and is determined by the measurement sampling interval. For a sampling frequency of 50 Hz, the vertical data density of a radio occultation is approximately 25 m.

From the discussions of "vertical resolution" associated with a single ray by Melbourne et al. (1994) and Kursinski et al. (1997), we may infer that the vertical scale  $Z$  of a single sounding depends on the first Fresnel zone of the GPS signals, which yields a diffraction-limited scale of approximately 0.2 km to 1.5 km in the troposphere and lower stratosphere. Although Gorbunov et al. (1996) and Gorbunov and Gurvich (1998) describe a "diffraction correction" technique, which reduces the size of the Fresnel zone and can improve (reduce) this scale, for the discussion here, we assume a nominal vertical scale of 1 km. This is also the order of the cross-track horizontal scale (Melbourne et al., 1994, p.90) and thus corresponds to the diameter of the tube depicted in Fig. 1.

The along-track horizontal scale  $L$  of an observation, which represents a weighted average of atmospheric properties along the path of the ray as depicted in Fig. 2, varies with the vertical scale  $H$  of the atmospheric feature (perturbation) being sampled (Gurvich and Sokolovskiy, 1985).  $H$  may range from a minimum limited by the vertical scale  $Z$  as defined above to the depth of the troposphere (8 km). From the geometry of the occultation sounding,  $L$  may be related to the vertical scale of the perturbation by

$$L = 2(2RH)^{1/2} \quad (1)$$

where  $R$  is the radius of the atmosphere at the ray tangent point (Gurvich and Sokolovskiy, 1985). For tropospheric applications  $R$  may be approximated by the mean radius of the Earth (6370 km) and (1) becomes

$$L \approx 225H^{1/2} \quad (2)$$

Thus for a shallow perturbation with vertical scale  $H$  of 1 km, the horizontal scale of the observation is of order 225 km. For a structure extending throughout the troposphere ( $H \approx 8$



km), the horizontal scale increases to approximately 640 km. Hence the horizontal scale (sometimes called the “along-track horizontal resolution” or simply the “horizontal resolution”) of a single occultation sounding is generally quoted as being between 200 and 600 km, with a typical value being 300 km.

It is misleading to interpret the horizontal scale as defined above as being a simple average of atmospheric properties along a path given by  $L$ . In reality, most of the information in a sounding is contributed by the atmosphere near the point of tangency, as shown in Fig. 2. As summarized by Melbourne et al. (1994, p. 90), “...the radio occultation technique for a single occultation recovers atmospheric refractivity profiles that are primarily derived from mesoscale-sized along-track averages.”

Although the horizontal averaging associated with radio occultation soundings may limit their value for some small-scale applications, several consequences of the averaging are actually advantages for initializing synoptic and subsynoptic scales of motion in NWP models and for climate studies. First, the averaging reduces the possibility of aliasing unrepresentative small-scale information from point-value, in situ observations from platforms such as radiosondes into the larger meteorologically significant scales of motion. In fact, the averaging properties of occultation soundings make them quite appropriate for accurately representing the scales of motion most relevant for initializing global models and for climate studies (Melbourne et al., 1994).

A second advantage of the relationship between horizontal and vertical scales represented by an occultation sounding is the consistency represented by these scales. Lindzen and Fox-Rabinovitz (1989) discuss the importance of a consistent vertical and horizontal resolution in both models and observations. They show that for middle and high latitudes, the ideal ratio of horizontal and vertical resolution in regional and global models is given by the ratio between vertical and horizontal scales

$$\frac{\Delta X}{\Delta Z} = \frac{N}{f_0} \quad (3)$$

where  $N$  is the Brunt-Väisälä frequency and  $f_0$  is the Coriolis parameter. Near the Equator the relationship between  $\Delta X$  and  $\Delta Z$  is given by

$$\Delta X^2 = \frac{Na}{2\Omega} \Delta Z \quad (4)$$

where  $a$  is the radius of the Earth and  $\Omega$  is the Earth's rotation rate. Lindzen and Fox-Rabinovitz (1989) estimate consistent resolutions for typical atmospheric conditions at the Equator, 22.5° and 45° latitude. Consistent ratios of  $\Delta X/\Delta Z$  for these latitudes are approximately 1700, 300 and 200 respectively, with values poleward of 22.5° typically 150 to 300.

The corresponding value of the ratio of minimum horizontal to vertical scales resolved by an occultation sounding from (2) with  $H=Z$  equals

$$\frac{L}{Z} \approx 225Z^{-1/2} \quad (5)$$

which ranges from about 225 for  $Z=1$  km to about 80 for  $Z=8$  km. Hence the ratios of horizontal to vertical scales of radio occultation soundings are fortuitously close to the ideal ratio for resolving synoptic and sub-synoptic-scales atmospheric features of interest. In contrast, Lindzen and Fox-Rabinovitz showed that for most NWP models and for satellite radiance data, the vertical resolution was far too low for consistency. With respect to observing systems, they note "Clearly, if observing systems with fine scale horizontal resolution are not accompanied by sufficient vertical resolution then phenomenon with fine horizontal scales will be incorrectly observed, and the observations will provide incorrect initial conditions for models." This latter condition appears to apply to present radiometric soundings from satellites, which have high horizontal resolution but relatively low vertical resolution. The addition of a global network of radio occultation soundings from COSMIC will therefore be highly complementary to the present satellite sounding system and the combined system will provide accurate and high-resolution global observations with excellent and consistent representation of the important horizontal and vertical scales of motion in the atmosphere.

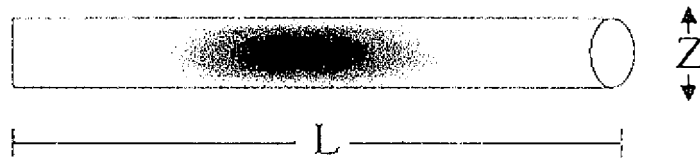


*Fig. 1.* Schematic depiction of tubular volume over which atmosphere contributes information to a single occultation phase (ray) measurement. The intensity of shading in the tube represents the relative weighting of atmospheric properties that contribute to the value retrieved at the center of the tube. For typical atmospheric structures,  $L$  and  $Z$  are approximately 300 and 1 km respectively.

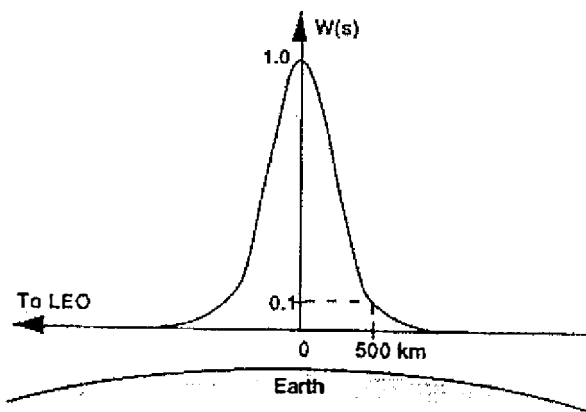


*Fig. 2.* Typical along-track weighting function for a single radio occultation measurement (from Melbourne et al, 1994). Most of the information is contributed by a mesoscale atmospheric volume centered at the ray tangent point.